Project No. 10-910

Alpha Radiolysis of Nuclear Solvent Extraction Ligands Used for An(III) and Ln(III) Separations

Fuel Cycle Research and Development

Stephen P. Mezyk
California State University, Long Beach

In collaboration with:
University of California, Irvine

Kimberly Gray, Federal POC
Leigh Martin, Technical POC

NEUP Nuclear Energy University Programs
U.S. Department of Energy

Alpha Radiolysis of Nuclear Solvent Extraction Ligands used for An(III) and Ln(III) Separations FY10-15 Final report

Fuel Cycle Research & Development

Prepared for
U.S. Department of Energy
NEUP Grant 10-910
Stephen P. Mezyk
California State University at Long Beach, CA
Bruce J. Mincher
Idaho National Laboratory, ID
Mikael Nilsson
University of California, Irvine, CA

01 August, 2016
DE-AC07-05ID14517

DISCLAIMER

This information was prepared as an account of work sponsored by an agency of the U.S. Government. Neither the U.S. Government nor any agency thereof, nor any of their employees, makes any warranty, expressed or implied, or assumes any legal liability or responsibility for the accuracy, completeness, or usefulness, of any information, apparatus, product, or process disclosed, or represents that its use would not infringe privately owned rights. References herein to any specific commercial product, process, or service by trade name, trade mark, manufacturer, or otherwise, does not necessarily constitute or imply its endorsement, recommendation, or favoring by the U.S. Government or any agency thereof. The views and opinions of authors expressed herein do not necessarily state or reflect those of the U.S. Government or any agency thereof.

CONTENTS

FIGURES

TABLES

SUMMARY

This document is the final report for the Nuclear Energy Universities Program (NEUP) grant 10-910 (DE-AC07-05ID14517) "Alpha Radiolysis of Nuclear Solvent Extraction Ligands used for An(III) and Ln(III) Separations". The goal of this work was to obtain a quantitative understanding of the impacts of both low Linear Energy Transfer (LET, gamma-rays) and high LET (alpha particles) radiation chemistry occurring in future large-scale separations processes. This quantitative understanding of the major radiation effects on diluents and ligands is essential for optimal process implementation, and could result in significant cost savings in the future.

The work performed here first measured and compared the impacts of γ and α- irradiation on ligands used in separation systems for nuclear material. Effort was focused upon the major ligands used in the PUREX, TRUEX and TALSPEAK processes, notably TBP, CMPO and DTPA. Electron pulse radiolysis experiments quantitatively determined reaction rate constants for these ligands with the most important radicals formed γ and α-radiation, which were the hydroxyl radical ($HO^{\bullet}$) and the nitrate radical ($^{\bullet}NO_3$) in the acidic aqueous phase and the $^{\bullet}NO_3$ radical and solvent radical cation ($C_{12}H_{26}^{+\bullet}$) in the organic (dodecane) phase. These data were augmented by steady-state irradiations on diluents and solvent systems, where distribution and stripping ratios and decomposition products were determined. While gamma irradiation was performed using either ^{60}Co or ^{137}Cs irradiators three distinctly different methods for alpha radiolysis were utilized. These included isotopic alpha irradiation (^{244}Cm, ^{243}Am, ^{211}At), helium ion beam irradiation (5.0 MeV He^{2+} accelerated particles) and a TRIGA™ reactor. As each of these alpha radiolysis systems had their own advantages and disadvantages they were used both simultaneously and independently on our systems in order to obtain the data of interest.

New findings from this work include the remarkable radiolytic stability of CMPO in dodecane, especially when in pre-contact with acidic water. This was attributed to the formation of a CMPO●HNO_3 complex that protected this ligand from radical degradation. Mass spectroscopy analysis of irradiated CMPO/dodecane systems showed different breakdown patterns and product distribution yields for the two forms of radiation, indicating that different reaction mechanisms were occurring. Comparison of the nitrate radical rate constants in the aqueous and the organic phase demonstrated that the latter were consistently faster. The measurements of the fast reaction kinetics of dodecane organic solvent radical cations with these extraction ligands was also performed, however, these data were not able to explain the stability of CMPO in this solvent. Hydroxyl radical reactions with metal-loaded DTPA in aqueous solution, and $^{\bullet}NO_3$ radical studies with CMPO-metal complexes showed that the reaction kinetics of metal-coordinated ligands was up to an order-of-magnitude faster. These kinetic findings were also seen in reactor based uranium-TBP radiolysis experiments, which showed that gamma irradiation caused generally much more degradation than alpha irradiation, and for both these forms of radiation, TBP complexed to uranium degraded far quicker than the free TBP ligand. Finally, a direct comparison of these three alpha irradiation techniques on a model dye system demonstrated that dose-rate effects were extremely important in quantifying the overall degradation efficiencies.

The knowledge gained in this work provides not only a comprehensive understanding of the radiation chemistry of currently proposed processes, but also give quantitative baseline information and evaluation methods for any future proposed nuclear solvent extraction systems. Thus this investigation filled major current gaps for real-world, irradiated, solvent systems.

1. INTRODUCTION

The development of a complete understanding of the fundamental chemistry of separations processes is essential for an optimized large-scale approach that will allow minimal processing and waste generation. These separations are designed to recover fissionable material and minimize the radiotoxicity of nuclear waste ultimately destined for geological disposal. The separation of the minor actinides, notably Americium, from dissolved nuclear fuel is one of the more formidable challenges in this regard. The partitioning of americium, and its subsequent transmutation in fast reactor fuel, would reduce high-level waste long-term storage requirements by as much as two orders of magnitude[1]. However, this is difficult to achieve as the lanthanides have very similar chemistry to americium, but cannot be incorporated into fuel.

Therefore, research into several aqueous solvent extraction processes for Ln(III) separation from An(III) is underway worldwide. In the USA the most developed process for this separation remains TALSPEAK[2] (Trivalent Actinide Lanthanide Separations by Phosphorus-reagent Extraction from Aqueous Komplexes) based on the competition between HDEHP (bis(2-ethylhexyl) phosphoric acid) in the organic phase and lactate-buffered diethylenetriamine pentaacetic acid (DTPA) in the aqueous phase. In Europe and Japan, more focus has been placed on the use of dithiophosphinic acids[3], diamide (DMDOHEMA)/bis(triazinyl)pyridine (BTP) mixtures and now diglycolamides[4]. A promising development now in the USA is the ALSEP process (Actinide Lanthanide Separations) which combines an organic phase containing DGA and phosphonic acid ligands, in competition with an aqueous phase containing a water soluble ligand to hold back actinides extraction[5].

For any large-scale separation process to be adopted, it must be robust under conditions of high-radiation does-rates and nitric acid hydrolysis. In particular, the effects of radiation on solvent extraction formulations may result in decreased ligand concentrations, giving lower metal distribution ratios, as well as reduced separation factors due to the generation of undesired complexing products, and impaired solvent performance due to films, precipitates, and increased viscosity[6]. As such, the quantification of the ligand degradation chemistry induced by the radiation field in which this separation will operate will provide useful information for future process design, and possible ways to avoid unwanted degradation products. While some work has been previously performed, or is currently underway towards this goal, significant gaps in our knowledge remain. Principal amongst these gaps are the effects of alpha-radiation and the kinetics/degradation products of irradiation of metal-loaded ligands. The study of alpha radiolysis impacts on solvents and particularly ligands was the focus of this NEUP-sponsored investigation.

This work originally proposed was to measure the effects of gamma and alpha irradiation on selected solvent systems using both steady-state irradiations, to measure effects on extraction performance (distribution and stripping ratios) combined with mass spectrometry to identify decomposition products, and electron pulse radiolysis measurements to determine the kinetic parameters for the important transient species reactions. Another focus was to investigate the radiolytically-induced degradation of metal-loaded ligands, particularly for the kinetics of these radiolysis reactions in the organic phase. Practically no work has been done in this media. Thus, our investigation aimed to fill several major gaps that are needed to describe the deleterious reactions that have importance in a real, irradiated solvent system. The knowledge gained in this study provides not only a comprehensive understanding of the radiation chemistry of currently proposed processes, but also give baseline information and evaluation methods for any future proposed nuclear solvent extraction systems.

2. SIGNIFICANCE

The fuel cycle research and development program has developed multiple aqueous solvent extraction processes for the separation of the actinides from used fuel. The main steps in USA proposals use TBP (tributylphosphate) in the PUREX (Plutonium Uranium Redox EXtraction) process for uranium extraction, octylphenyl-N,N-diisobutylcarbomoyl-methylphosphine oxide CMPO in TRUEX (TRansUranic EXtraction) for group lanthanides and trivalent actinide removal, and then HDEHP/DTPA in the conventional TALSPEAK process[2] for the separation of the trivalent actinides and lanthanides. Several TALSPEAK-like alternatives are also under consideration.[5] As the most mature process, the radiation chemistry of PUREX has been the most thoroughly investigated, and is best understood. The TRUEX process has received less attention, and little radiation chemistry work has been performed for TALSPEAK. Apart from TBP, almost no work has been done on the alpha radiolysis of any of these solvent (diluent plus extraction ligands) systems. Since all these systems will be exposed to high gamma and alpha radiation doses, and solvent recycling is desirable to minimize process costs, an understanding of the major radiation effects is necessary for their successful deployment. Minimizing deleterious effects with proper design of ligands and solvent washing steps to remove radiolytic degradation products, could result in significant cost savings.

3. APPROACH

The initial focus was on TBP and CMPO, the most important ligands in the U.S. recycling strategy. Even though TBP radiation-induced chemistry had been studied for many years it is important to recognize that little alpha-radiolysis information was available, and the results generated here for both ligands would be new. The comparison of alpha and gamma irradiations would also allow us to elucidate the mechanisms of ligand decomposition, as the respective yields of radicals produced by the different radiation sources are known. It is also important to note that the radical kinetics do not depend on how the radicals are produced, the main difference between alpha and gamma radiolysis is in the yields of those radicals. Thus the data obtained by pulse radiolysis methods are applicable to both alpha and gamma radiolysis. Once the optimal techniques were established with TBP and CMPO additional studies on other ligands such as HDEHP and DTPA were envisioned. The structures of these main ligands that were investigated are shown in Figure 1. All these results and techniques established here are applicable to other ligand systems as well, and thus these results remain useful as new solvent systems are developed.

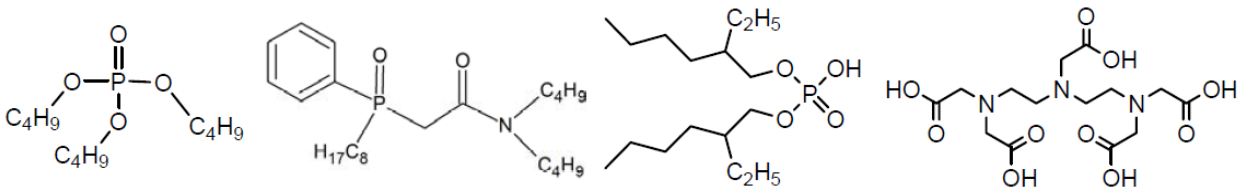

Figure 1. Ligands of interest in this study. From left to right: TBP, CMPO, HDEHP, and DTPA

4. RESULTS

4.1 Alpha radiolysis measurements

The determination of alpha-radiolysis induced ligand degradation is difficult, with no single reported method being optimal. Therefore, in this study we conducted our experiments using three concomitant approaches to perform these desired measurements and to identify the best method. The three complementary methods were:

4.1 a) Internal isotope irradiation: Selected ligands were alpha-irradiated using ^{244}Cm in 0.10 M HNO_3 as an internal source at Idaho National Laboratory. Absorbed dose ranges were achievable up to 500 kGy, similar to the absorbed doses achieved using analogous gamma-irradiation experiments, which allowed direct comparison of dose constants, yields, and decomposition products between the two isotopic radiation sources. These experiments were of long duration, typically weeks of irradiation with samples withdrawn at appropriate intervals for testing. The advantages of this approach were that large accumulated doses were available, plus that ligand/solvent systems were irradiated in the same manner that would be experienced for large-scale, reprocessing, conditions. A significant disadvantage of the use of isotopic irradiations was that the resulting samples were alpha-emitter contaminated, which limited the analytical techniques available for the determination of ligand decomposition products. The analytical suite of techniques we were able to use for these contaminated samples included HPLC, UV/Vis spectroscopy and ICP-MS.

Another approach was use of the alpha-emitting isotope ^{211}At. These experiments were performed in collaboration with Chalmers University of Technology in Gothenburg, Sweden, who had a ready supply of this medical isotope from Copenhagen. The ^{211}At isotope was produced by irradiation of bismuth targets with high-energy alpha particles. This isotope has a 7.2 hour half-life, emitting alpha particles with an average energy of 5.98 MeV, decaying either through ^{207}Bi or ^{211}Po to stable ^{207}Pb[7]. The complete α-decay of this isotope occurred within a few days, which considerably simplified post-irradiation analytical chemistry. As we were unable to procure a source of this isotope in the US, we performed four experiments at Chalmers Technical University over the period of this grant. While this approach afforded significantly more options in post-irradiation analysis, one major disadvantage was that only low (20-50 kGy) total doses could be obtained. Often, this energy was just not sufficient to cause significant ligand degradation.

4.1 b). Helium ion-beam measurements: The use of alpha particle accelerators allows the continuous irradiation with alpha particles on aqueous, organic and mixed biphasic systems, with selected alpha energies at much larger dose rates (~10 kGy/hour) than from internal sources, and no residual activity. The latter is the most significant advantage of this approach, allowing for standard analytical techniques to be used on these irradiated samples. As such, we utilized the accelerator system at the University of Notre Dame to perform irradiation experiments on different solvent/solute systems[8]. However, one drawback to this irradiation method is that the α-particles have limited solution penetration (~30 μm) due to their 5 MeV energies after passing through the cell window. This meant that cell contents had to be stirred vigorously. Experiments had to be conducted to establish optimal conditions for this stirring, but were ultimately successful. In addition, while much larger dose rates were available compared to the isotopic irradiations, the scheduling of beam time on the accelerator meant that only relatively low doses (50-100 kGy total dose) could be achieved for only a small number of samples.

4.1 c) Reactor for neutron induced alpha decay: A new, novel, approach to elucidating alpha-radiolysis effects that we incorporated into this study was to utilize the same principle used in Boron Neutron Capture Therapy (BNCT) to create a significant alpha dose within a solution. Solutions were placed inside a sealed vessel that also contains a significant amount of boron-10, that would capture reactor-generated neutrons in the TRIGA™ reactor at the University of California Irvine and undergo alpha decay to lithum-7; $^{10}B(n,\alpha)^{7}Li$[9]. The total energy of the reaction is ~2.79 MeV and is shared by the alpha particle (~1.47MeV), the ^{7}Li recoil nucleus (~0.84 MeV), and in 94% of the reaction events there was also a 0.48 MeV gamma ray emitted[10] (see Figure 2).

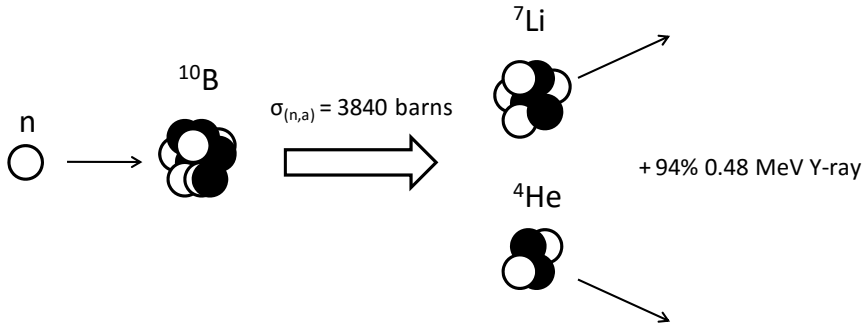

Figure 2. Schematic of the $^{10}B(n,\alpha)^{7}Li$ reaction used in the TRIGA™ reactor at University of California, Irvine for these high LET alpha irradiation experiments[10].

Both the alpha particle and the Li recoil represent high LET decay modes that mimic conditions anticipated for spent fuel reprocessing. The presence of the gamma ray is not seen as a major problem as their effects can be accounted for by separate experiments. The major advantage to this approach was that it allowed us to investigate both the effect of total alpha dose to a sample as well as the effect of dose rate. However, these studies required careful calibration of the dose rates and correlations needed to be made to account for effects from gamma doses due to the vicinity of the reactor core.

The goal of performing these three different types of alpha-radiolysis was to quantitatively evaluate the radiation induced degradation of both free and metal-loaded ligands, and to establish the most efficient and cost-effective approach in obtaining the required data. Combining these alpha radiolysis data with the auxiliary gamma studies, and ultimately bench-scale distribution measurements on irradiated systems, the ultimate aim of this work was to provide information that would allow creation of a predictive computer model that could be ultimately used to model process conditions to optimize extraction ligand performance in separating An(III) and Ln(III). Our overall approach in this project is summarized in Figure 3.

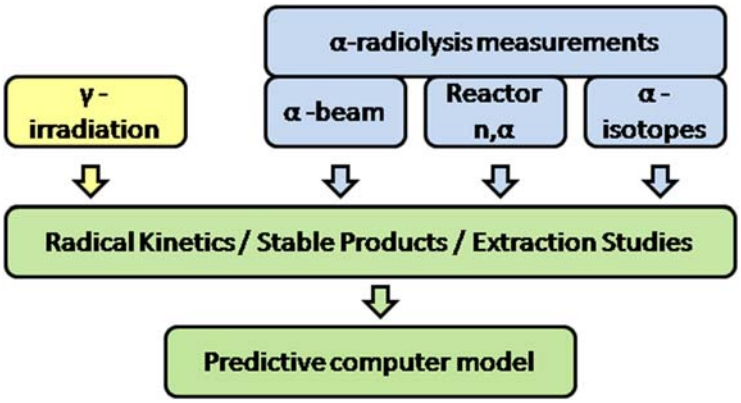

Figure 3. Summary of overall experimental approach used in our NEUP study.

4.2 CMPO studies

4.2.1 HPLC measurements

The ligand chosen for initial study was CMPO (octylphenyl-N,N-diisobutylcarbomoyl methyl-phosphine oxide) in dodecane. Dodecane was used throughout this entire study to mimic the organic diluents used for large-scale reprocessing. To achieve post irradiation quantification of CMPO a high performance liquid chromatography (HPLC) method for its measurement in dodecane that featured a low pH buffer, octanol as a co-solvent with 2-propanol, and ultraviolet (UV) detection was developed[11]. All experiments were carried out isocratically, using a mixture of 30 mM phosphate buffer, pH~2.6, and 2-propanol with 3.6% 1-octanol in 60/40 ratio. The chromatographic separation was achieved with a C18 reverse-phase (RP-C18) column (Supelco, 25 cm × 4.6 mm, 5 μm) with a flow rate of 1 mL/min. The column temperature was maintained at 50°C. CMPO concentrations were determined at a wavelength of 220 nm, the peak of its UV absorption spectrum.

Validation data indicated that the HPLC–UV method for CMPO determination provided good linearity, sensitivity, accuracy and precision. To extend this methodology to the measurement of CMPO/ dodecane solutions for conditions that anticipated nuclear fuel reprocessing, we used 100 mM CMPO in dodecane contacted with 3–5 M HNO_3 before being subjected to gamma irradiation. As a typical example[11], Figure 4 shows CMPO samples γ-irradiated in the presence of 3 M HNO_3. Analysis of the sample receiving a dose of 229.8 kGy showed peaks corresponding to HNO_3 (the initial peak), TPP (triphenyl phosphate, the internal standard) and CMPO, and a significant radiolysis product at 10.5 min that was shown to correspond to mono-isobutyl CMPO by subsequent ESI-MS experiments. In addition, lower abundance peaks were seen at ~6 min, 14–15 min, and 25–30 min (regions a, b, c in Figure 4) that are very likely other radiolysis products. This conclusion is supported by the chromatograms generated for a sample treated with a higher dose (612.8 kGy), which showed marked increases in the responses of the low abundance peaks, including the mono-isobutyl CMPO derivative and significant decrease in the CMPO concentration. Other radiolysis products identified by GC in this study, and previously[12,13], included octylphenylphosphinic acid and the corresponding isopropyl ester, octylphenylphosphinyl acetic acid, and octylphenyl (N-isobutyl) carbamoyl-methylphosphine oxide.

Further evaluation of our HPLC–UV method was conducted to analyze unirradiated CMPO samples that were pre-contacted with HNO_3. The effect of HNO_3 on unirradiated CMPO was also of interest because it is known that CMPO complexes and extracts acid as well as metals. A previous study by Fuji *et al.*[14] showed apparently decreasing CMPO concentration with increasing acidity at low [HNO_3], up to 3 M, but that the measured CMPO concentration appeared to be insensitive to higher acid concentrations. In our work, equal volumes of 100 mM CMPO in dodecane were contacted with different concentrations of HNO_3, after which the separated dodecane layer was analyzed by our standard CMPO method. Figure 5 shows the effect of HNO_3 on the UV response at 220 nm. Our experiments agreed well with Fuji et al.'s[14] studies at low HNO_3 concentration. However, at higher nitric acid concentrations the apparent CMPO concentration continued to decrease to the maximum acid concentration of 6 M. It was suspected that the reason for the apparent decrease in CMPO concentration in the presence of acid was due to the formation of a complex, $(2HNO_3 \cdot CMPO)_{org}$[14]. Their conclusion was in qualitative agreement with earlier work,[15,16] however, the prior studies had concluded that the stoichiometry of the complex was $(HNO_3 \cdot 2CMPO)_{org}$.

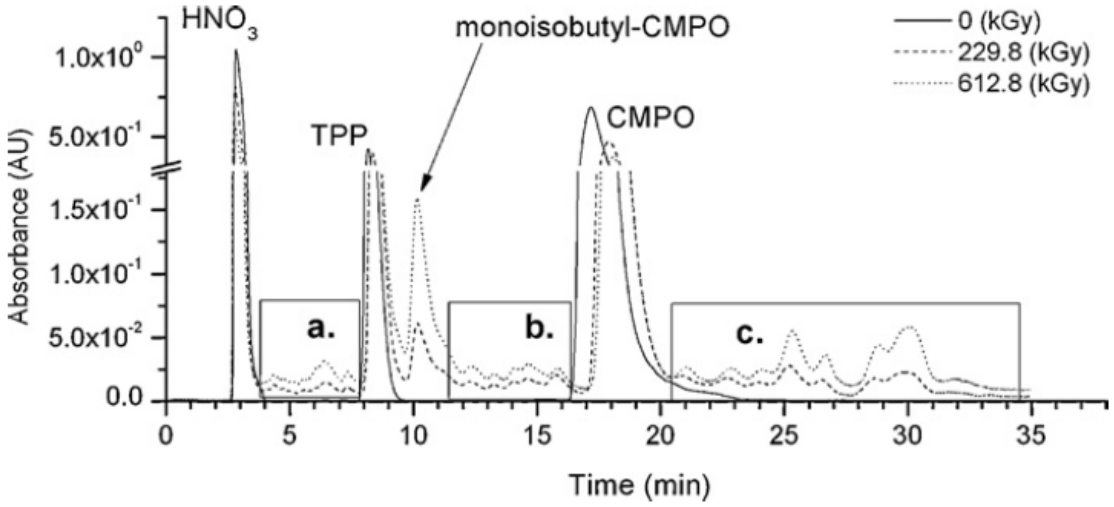

Figure 4. HPLC–UV chromatograms of γ– irradiated CMPO with a non-irradiated control. UHPLC/ESI-MS showed mass 352 as a main radiolysis product. Lower abundance peaks were seen at ~6 min, 14–15 min, and 25–30 min (regions a, b, c) that are very likely other radiolysis products.

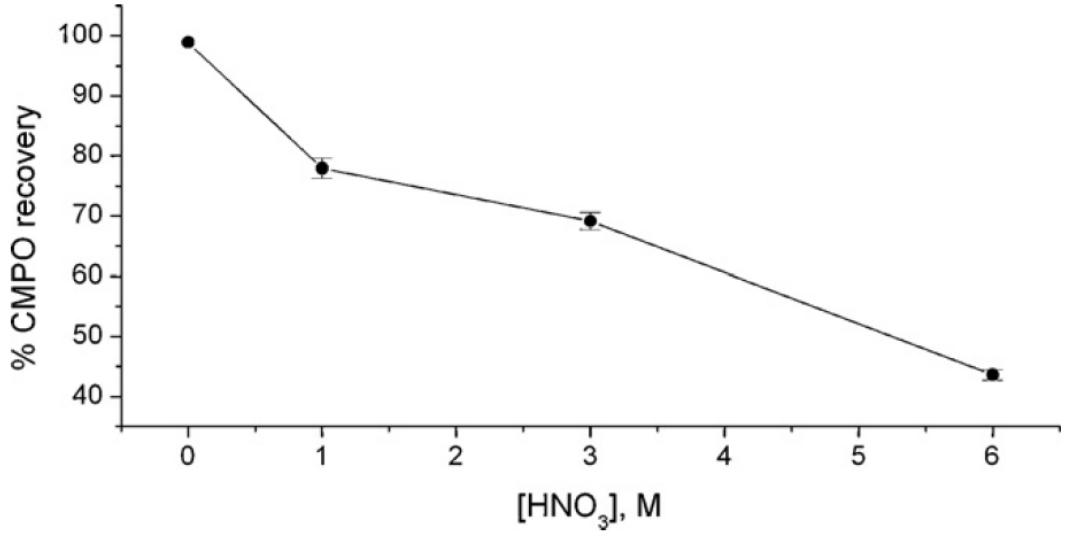

Figure 5. Ratio of free CMPO concentration to initial concentration of CMPO as a function of [HNO_3]. CMPO in dodecane was determined by HPLC. Errors shown are the standard deviation of duplicate measurements.

To further attempt to elucidate the formation of these complexes, which would considerably impact the measurements of CMPO concentrations in later studies, direct infusion ESI-MS was conducted in this study in to directly observe the suspected complex. Both the acid extract of HNO_3-contacted CMPO and the organic layer produced an abundant ion at m/z 900 (Figure 6) in addition to the expected $[CMPO+H]^+$ at m/z 408. The m/z 900 ion would nominally correspond to $[(CMPO)_2(HNO_3)Na]^+$, a conclusion supported by collision induced dissociation (CID) which produced a single fragment ion at m/z 837, corresponding to elimination of 63 Da (loss of HNO_3). These results support the existence of a complex

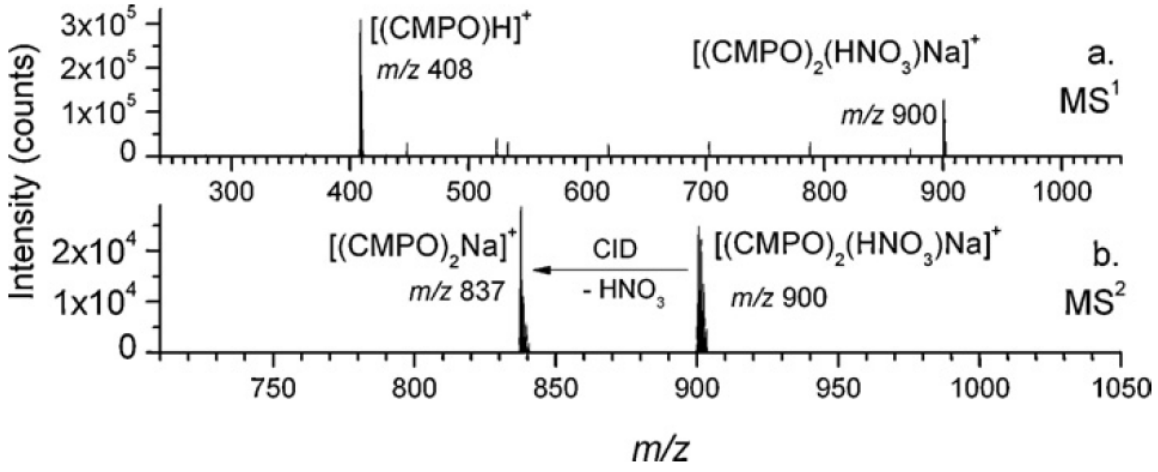

Figure 6. (a) MS1 of the acid extract of CMPO contacted with HNO_3. (b) MS2, isolation and collision induced dissociation of m/z 900.

having a 2:1 ratio of CMPO:HNO_3. Ions that would correspond to a 1:2 stoichiometry were not observed. The implications of the formation of this complex that is apparently undetectable by HPLC is that standard calibration curves should be prepared by contacting known concentration CMPO solutions with the appropriate acid concentration just prior to analysis.

4.2.2 ^{60}Co gamma and alpha irradiation of CMPO in dodecane

The ^{60}Co gamma irradiation of 100 mM CMPO solutions in dodecane was conducted at Idaho National Laboratory, utilizing their Gammacell-220 irradiator, and at the University of Notre Dame Radiation Research Laboratory, using three different ^{60}Co irradiators with various dose rates. These solutions were irradiated under different conditions, to further elucidate the chromatographic findings detailed in the previous section. Figure 7 shows a summary of our measured data for irradiated sealed samples. The pre-contacted CMPO/dodecane irradiations showed an apparent lower initial yield, consistent with the chromatography results above. For both dry and pre-contacted CMPO/dodecane irradiation, no difference in ^{60}Co dose rate over the range 0.175 – 15.9 kGy hr^{-1} was seen. The decay of CMPO was linear with dose, implying zero-order kinetics. From the slope of this line, a *G*-value for CMPO loss of $-G_{CMPO} = 0.145 \pm 0.008$ μM Gy^{-1} was obtained (minus sign corresponds to ligand loss). The corresponding slope for the ^{60}Co gamma irradiated pre-contacted solution was much lower, $-G_{CMPO} = 0.034 \pm 0.017$ μM Gy^{-1} showing that there is significant radioprotection from the nitric acid contact which reduced the rate of CMPO degradation. It is also important to note that the low $-G_{CMPO}$ value for the pre-contacted solution data is heavily influenced by the two end-point values, which suggests that the CMPO concentration change could be effectively zero (within 2σ). Subsequent experiments demonstrated that water contact alone did not give any protection, and that having air continuously bubbled through the solutions during irradiation also slowed down the overall degradation.

More interesting are the alpha radiolysis results. The ion-beam data for the dry solvent falls directly on the ^{60}Co irradiation line, which was not anticipated as the radiolysis of organic diluent by the two different forms of irradiation are very different. Similar results were found for the acid pre-contacted data, where the 0.10 M HNO_3 ^{244}Cm data was consistent with the 3.0 M HNO_3 γ-irradiated data? In water, the radiation-induced decomposition occurs via[17]:

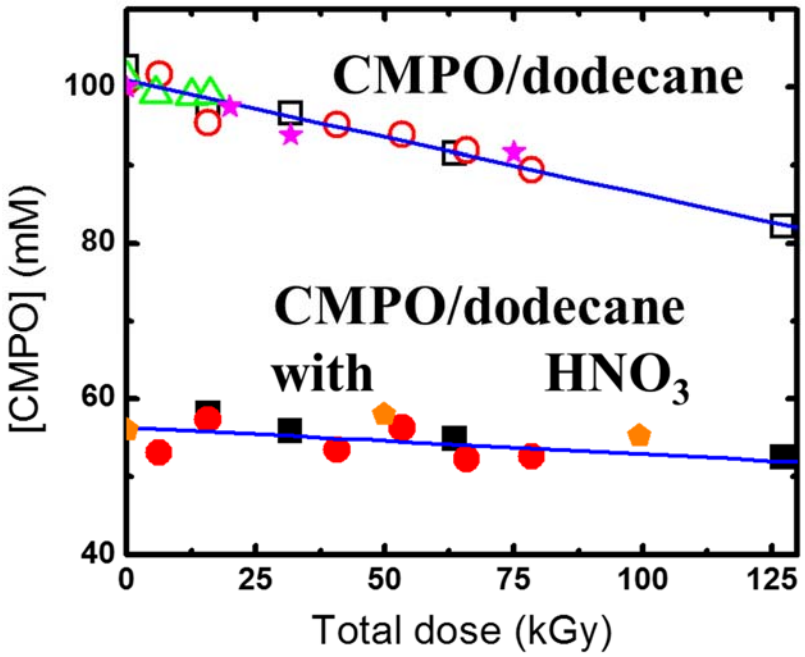

Figure 7. Summary of CMPO degradation measured using ^{60}Co irradiation (0.175 (Δ), 3.14 (O,●) and 15.9 (□, ■) kGy hour^{-1}) and helium ion beam radiolysis (✱) and ^{244}Cm alpha irradiation (⬟). Open symbols correspond to dry CMPO/dodecane while solid symbols correspond to CMPO pre-contacted with HNO_3 (3.0 M for γ irradiations, 0.10 M for ^{244}Cm α irradiations). Solid lines correspond to calculated γ *G*-values (degradation efficiencies) of $-G_{CMPO} = 0.145 \pm 0.008$ and $-G_{CMPO} = 0.034 \pm 0.017$ mM kGy^{-1} (μmol Gy^{-1}) for dry and pre-contacted solutions, respectively.

$$H_2O \xrightarrow{radiation} [0.28]HO^\bullet + [0.27]e_{aq}^- \; [0.06]H^\bullet + [0.07]H_2O_2 + [0.27]H_3O^+ + [0.05]H_2 \qquad (1)$$

where the numbers in brackets are the *G*-values of each species in μmol per Gray (or per Joule in water) of energy deposited[17]. These yields are given for low linear energy transfer (low LET) radiation, such as γ-rays, electrons or X-rays for water in the pH range 3-10. At the more acidic conditions of both these experiments, and under anticipated large-scale process conditions, the hydrated electrons formed (e_{aq}^-) would quickly react with H_3O^+ to give more hydrogen atoms ($H^\bullet$)[17]:

$$e_{aq}^- + H_3O^+ \rightarrow H_2O + H^\bullet \qquad k_2 = 2.3 \times 10^{10}\ M^{-1}\ s^{-1} \qquad (2)$$

In addition, at high concentrations of HNO_3 in the water direct radiolysis of this chemical also gives the nitrate radical ($NO_3^\bullet$):

$$HNO_3 \xrightarrow{radiation} NO_3^\bullet + H^\bullet \qquad (3)$$

The nitrate radical can also be formed indirectly through the radical reaction of the hydroxyl radical ($HO^\bullet$) with undissociated nitric acid[18]:

$$HO^\bullet + HNO_3 \rightarrow NO_3^\bullet + H_2O \qquad k_4 = 1.4 \times 10^{8}\ M^{-1}\ s^{-1} \qquad (4)$$

In the presence of dissolved oxygen some hydrogen atom loss through the formation of relatively inert $HO_2^\bullet$ radicals will occur[17]:

$$H^\bullet + O_2 \rightarrow HO_2^\bullet \qquad k_5 = 1.2 \times 10^{10}\ M^{-1}\ s^{-1} \qquad (5)$$

but the relatively low dissolved oxygen concentration will not be sufficient for quantitative removal. Thus under acidic aqueous conditions the main ligand degradation species are the hydroxyl ($HO^\bullet$) and nitrate ($NO_3^\bullet$) radicals. Some hydrogen atom ($H^\bullet$) may also occur depending upon the amount of dissolved oxygen. Acid pre-contacted organic solvent (dodecane) radiolysis will give the same species, plus additional organic carbon-centered radicals and solvent radical cations. The carbon-centered radical species will also react with oxygen species to produce less reactive peroxyl compounds ($RO_2^\bullet$). Like $HO_2^\bullet$ the $RO_2^\bullet$ species are unlikely to influence ligand degradation significantly.

The alpha radiolysis of water and organic solvents has been shown to give the same radical and molecular product species, but in different initial yields. In general, the amount of radicals produced is lower, and the amounts of molecular products higher. For example, in acidic water the ^{210}Po 5MeV α radiolysis gives[19]:

$$H_2O \xrightarrow{\alpha\ radiation} [0.05]HO^\bullet + [0.33]H^\bullet + [0.15]H_2O_2 + [0.16]H_2 \qquad (6)$$

Moreover, separate experiments with H_2O_2 contact showed no change in CMPO concentration over a one-week period indicating this was not a major degradation pathway. Ultimately, the major species involved in the degradation of separations ligands in mixed-phase solutions will be the three radicals $HO^\bullet$, $NO_3^\bullet$ and perhaps $H^\bullet$. It is their chemistry that is of major significance in both α and γ irradiated solution, and since their yields are different gamma and alpha radiolysis would be expected to give different results. While this was observed for the ^{244}Cm experiments (practically no CMPO degradation measured), the agreement between the dry dodecane irradiation data remain puzzling.

To further elucidate the chemistry of CMPO/dodecane degradation and protection, additional ^{60}Co experiments were conducted on CMPO/dodecane solutions that were pre-contacted with acidic water[20]. The γ-irradiation of 0.1 M CMPO/dodecane in contact with an equal volume of 0.1 M HNO_3 was consistent with that of pure organic solution, at about $-G_{CMPO} = 0.18$ μmol J^{-1}, again confirming that the protection of CMPO using 3 M HNO_3 must result from the nitric acid itself, and not merely from the presence of water. Additional experiments confirmed that nitrate ions alone also did not confer any degree of protection. The variation of $-G_{CMPO}$ with pre-contact acidity is shown in Figure 8.

This linear decrease observed for increasing acidity pre-contact allows us to calculate a pseudo-equilibrium constant for the formation of a $[CMPO_x\bullet(HNO_3)_{y+1}]$ complex. This complex is written in this fashion as its exact stoichiometry is not known. However, it is clear that with increasing acidity, we appear to be adding more HNO_3 to an initial $[CMPO_x\bullet(HNO_3)_y]$ complex formed at lower HNO_3 concentrations (hence y → y+1). Writing this addition reaction simply as:

$$[CMPO_x\bullet(HNO_3)_y](org) + HNO_3(aq) \leftrightharpoons [CMPO_x\bullet(HNO_3)_{y+1}](org) \qquad K_7 \qquad (7)$$

and using the equilibrium constant K_7 and mass balance the total $[CMPO]_{total}$ from the apparent measured value, $[CMPO]_{meas}$, can be calculated using the expression:

$$\frac{[CMPO]_{total}}{[CMPO]_{meas}} = f_{CMPO} = 1 + K_7[HNO_3(aq)] \qquad (8)$$

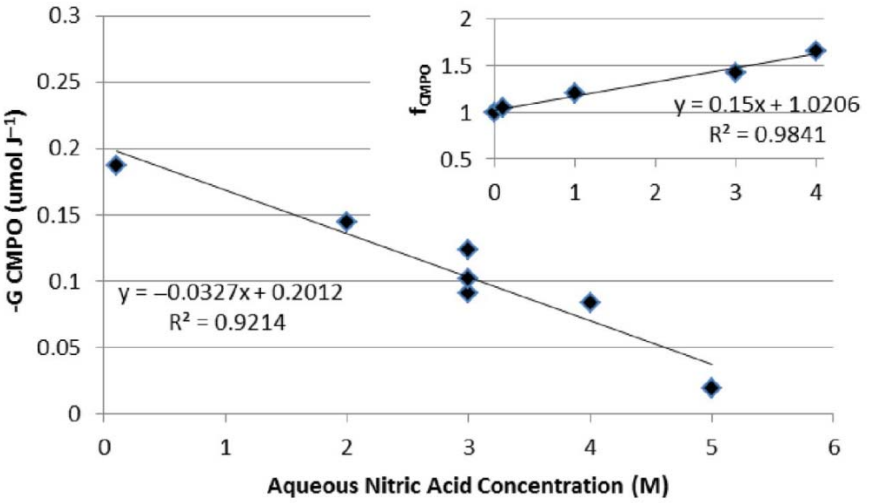

Figure 8. The decrease in $-G_{CMPO}$ for the irradiation of 0.1M CMPO in contact with aqueous phases of increasing nitric acid concentrations. The mean of three determinations at 3 M HNO_3 was 0.073 ± 0.012 μmol J^{-1}. Inset: Determination of equilibrium constant for $[CMPO_x \bullet (HNO_3)_{y+1}]$ complex formation.

From the data plotted in the Figure 8, Inset, $K_7 = 0.150 \pm 0.011$. This value is about an order of magnitude lower than that for CMPO•HNO_3 formation in trichloroethylene[16]. Moreover, such a relatively low equilibrium constant suggests that the product complex should dissociate in the HPLC eluent, which implies that this equilibrium is not just for a single HNO_3 molecule being complexed to only CMPO. Further experiments are planned to determine the true complex composition.

4.2.3 ^{60}Co Irradiated CMPO/dodecane Solvent Extraction Experiments

Post-irradiation CMPO solutions were used for Am solvent extraction experiments[20]. Equal volume, room temperature (21 ± 2◦C) forward extraction contacts of 2 min duration were performed from ^{243}Am traced 2 M HNO_3. The tracer concentration was ~2 μM Am. As these experiments were performed in the absence of TBP, it was found that CMPO, and its metal complexes, have relatively low solubility in dodecane. Thus the irradiated 0.1 M CMPO solution was diluted to 0.016 M CMPO with fresh dodecane prior to use, to improve the solubility of the extracted Am•CMPO complex. However, third-phase formation and poor mass balances still accompanied some irradiations, due to the low solubility of radiolysis products and radiolysis-product complexes with Am (see Figure 9).

Following contact, 1 mL aliquots of each phase were removed for γ-ray counting, with the Am activity determined at 74.7 keV. The loaded organic phase was then stripped with an equal volume of 0.1 M HNO_3, and aliquots of these phases removed for γ-counting. The distribution ratio (D_{Am}) was determined as the ratio of Am activity in the organic to aqueous phases. Thus, high values for the forward extraction D_{Am} indicate favorable solvent extraction, while low values for the strip D_{Am} indicate favorable back-extraction. All extractions were performed in triplicate, with the reported D_{Am} being the mean results. The low CMPO concentrations necessitated by low CMPO solubility resulted in low distribution ratios, with only limited activity transferred to the organic phase. Thus, the precision of the strip distribution ratios was limited, with relative standard deviations for replicate measurements as high as ± 20%. The precision of the triplicate forward extractions averaged ± 5%.

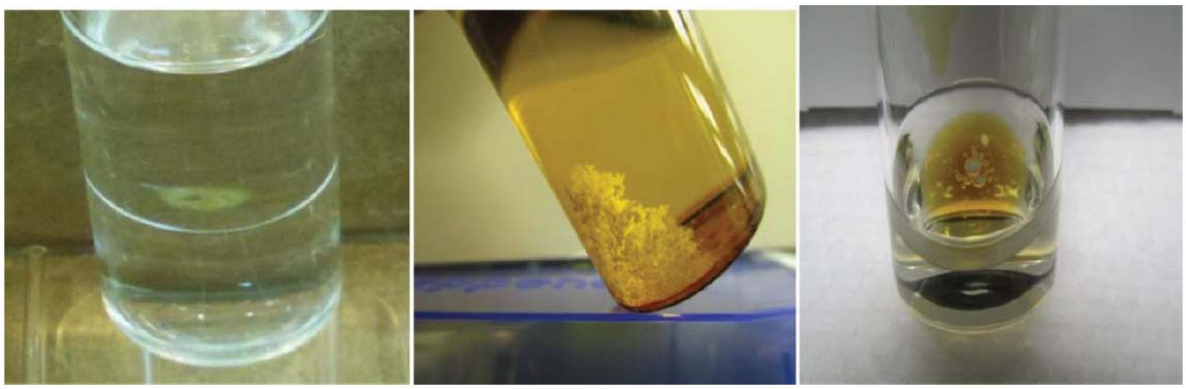

Figure 9. (Left: Third-phase formation when Am solvent extraction was performed using 0.1 M CMPO/dodecane irradiated in the presence of 0.1 M HNO_3 solution. The solution was diluted to 0.016 M in CMPO with fresh dodecane prior to the extraction contact. Middle: Precipitate formed when samples of 0.1 M CMPO/dodecane were irradiated in the absence of a bulk aqueous phase with no metal present. Right: Third-phase formation when 0.1 M CMPO/dodecane was irradiated in the presence of 2 M HNO_3, for both deaerated and air-sparged samples in the absence of metal.

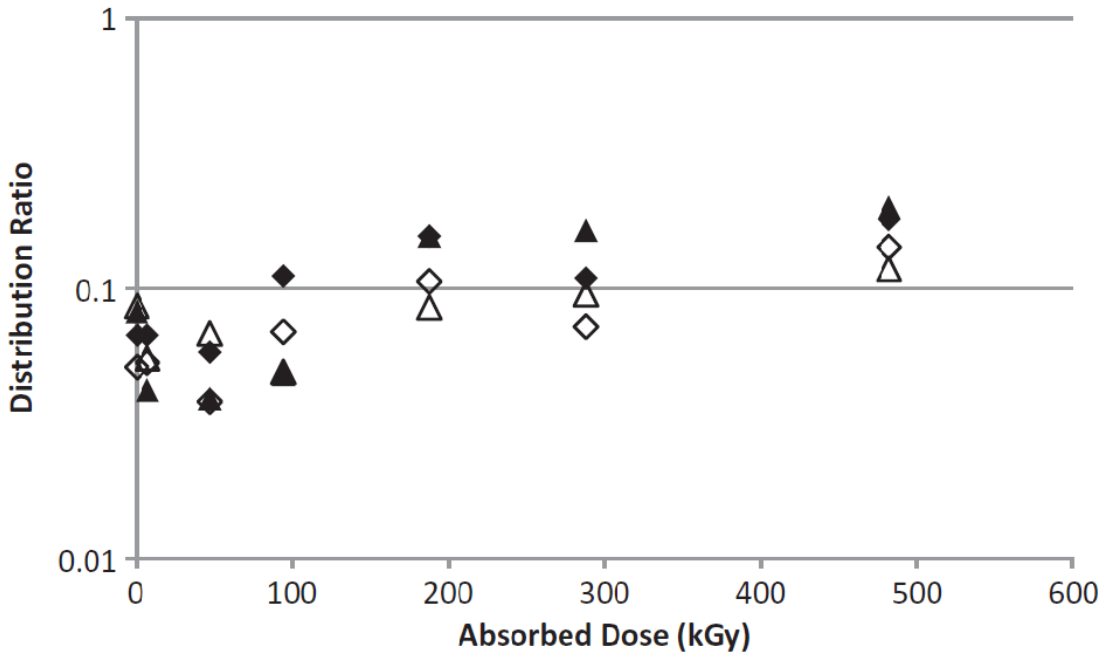

Figure 10. Americium distribution ratios for extraction from 2 M HNO_3 (closed symbols), and stripping of the loaded organic phase (open symbols) using 0.1 M HNO_3, for irradiated 0.1 M CMPO/dodecane solutions. The CMPO solution was irradiated in the absence of an aqueous phase (diamonds) or in contact with an equal volume of 0.1 M HNO_3 (triangles), then diluted to 0.016 M prior to the extractions.

As shown in Figure 10, irradiations in the absence of an aqueous phase, or in contact with an equal volume of 0.1 M HNO_3, resulted in an increase in both the forward extraction and stripping distribution ratios for Am. Both increased by nearly a factor of two at the highest absorbed dose of 482 kGy. A comparison of the neat and 0.1 M HNO_3-contacted irradiated systems showed that the concentration of

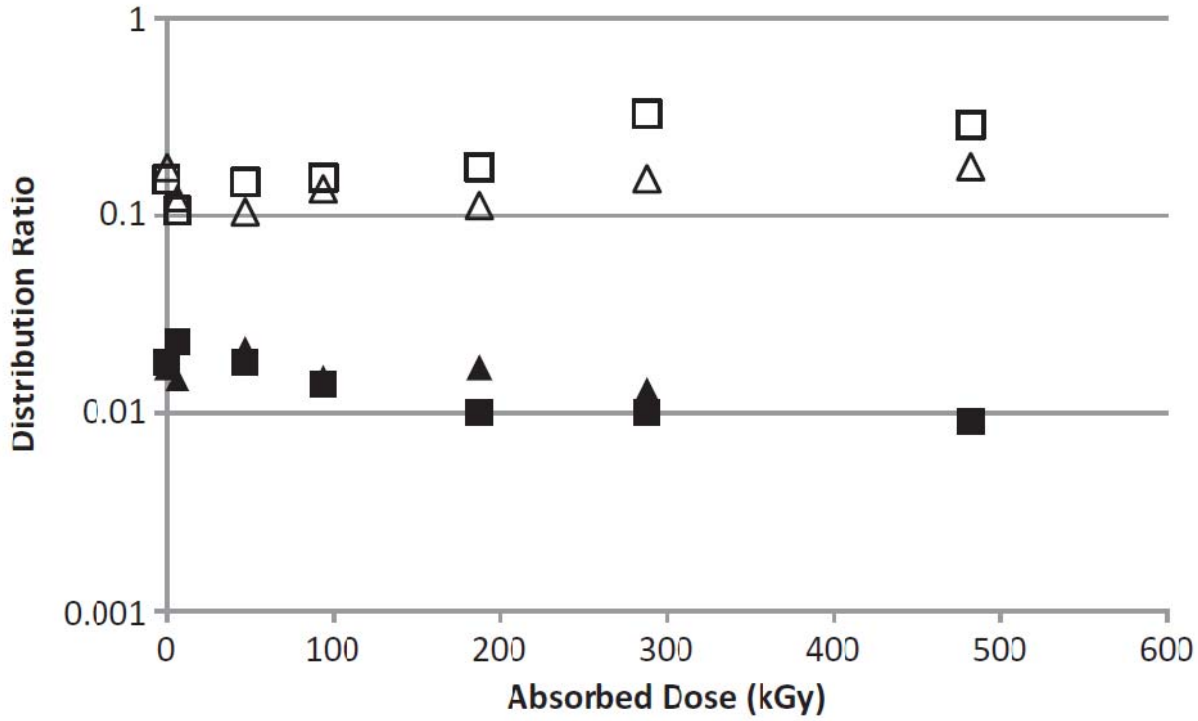

Figure 11. Americium distribution ratios for extraction from 2 M HNO_3 (closed symbols), and stripping of the loaded organic phase (open symbols) using 0.1 M HNO_3, for irradiated 0.1 M CMPO/dodecane solutions. The CMPO solution was irradiated after pre-equilibration with 2 M HNO_3 (triangles), or in contact with an equal volume of 2 M HNO_3 (squares), then diluted to 0.016 M prior to the extractions.

CMPO decreased while the extraction and stripping distribution ratios increased. This implies that the irradiation of CMPO/dodecane and CMPO/dodecane in contact with dilute acid have similar effects on $-G_{CMPO}$ and solvent extraction, indicating that degradation products capable of complexing Am are produced by radiolysis under both conditions. Furthermore, the mass balances quickly deteriorated for the forward extractions shown in Figure 10, until at the highest absorbed dose only ~75% of the initial Am was accounted for in the two post-extraction phases. This was accompanied by the appearance of a third phase, and/or precipitate, as shown in Figure 9. We attribute this third phase to the production of an Am radiolysis product complex that has limited solubility in either phase. However, it did not appear for irradiations at higher acidities, indicating that the protonated version of the product is soluble in the aqueous phase.

When 0.1 M CMPO/dodecane was irradiated in contact with higher nitric acid concentrations, stripping distribution ratios from the loaded organic phase also increased; however, forward extraction distribution ratios decreased. These results agreed with previous investigations[21-23] and are shown in Figure 11 for irradiation of 0.1 M CMPO irradiated in contact with an equal volume of 2 M HNO_3, or after pre-equilibration with 2 M HNO_3 but irradiation of only the wet organic solution. Pre-equilibration produced the same effect on solvent extraction, as did the bulk acid phase. Additionally, even for the non-irradiated samples the strip distribution ratios were higher than the forward extraction distribution ratios. This was produced by low forward extraction D_{Am}, as compared to those in Figure 10 and is attributed to competition for the rather low CMPO concentration by nitric acid. Continued increases in nitric acid

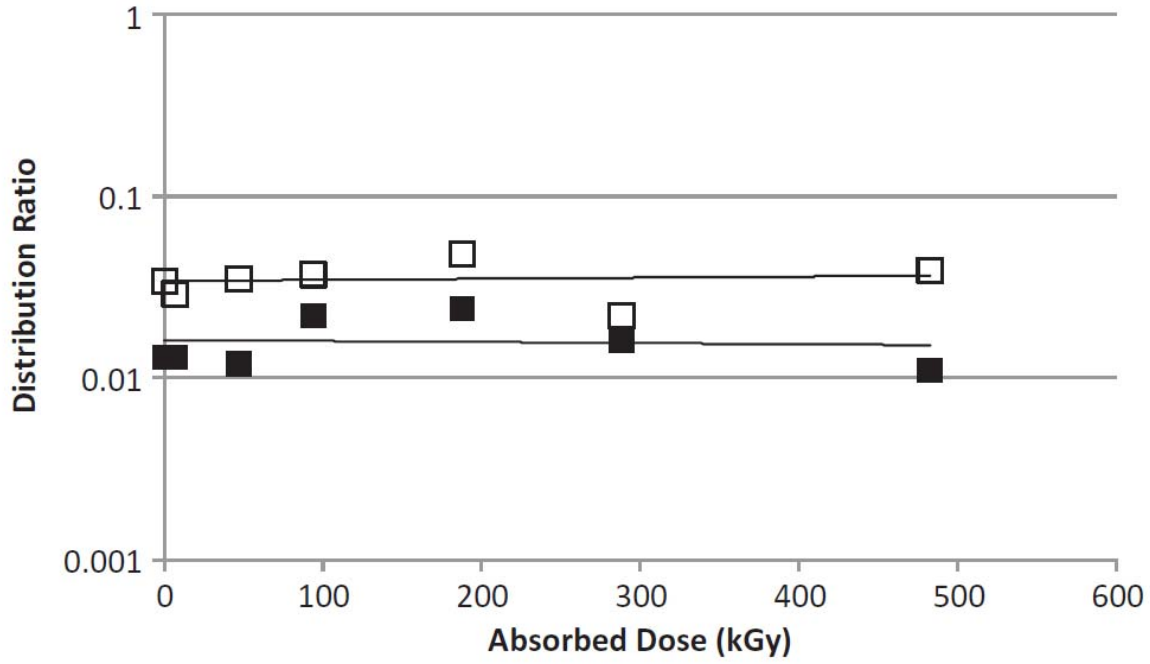

Figure 12. Americium extraction from 2 M HNO_3 (closed squares) and stripping from the loaded organic with 0.1 M HNO_3 (open squares) for 0.1 M CMPO/dodecane γ-irradiated in aerated contact with an equal volume of 2 M HNO_3. The CMPO was diluted to 0.016 M prior to extractions.

concentration had no further effect on Am extraction or stripping, despite the changes in $-G_{CMPO}$ shown in Figure 8. These results indicate that a product with high affinity for Am is produced that becomes complexing only upon contact with the dilute acid phase used in stripping. This effect had been previously reported, and is usually attributed to acidic decomposition products that are soluble in the organic phase[12,23,25].

Irradiated neat organic samples and organic samples that had been pre-equilibrated with 2 M HNO_3 but contained no bulk aqueous phase produced a white precipitate in greater amounts with increasing absorbed dose. The precipitate did not appear when samples were irradiated in contact with a bulk aqueous phase. The insoluble product, as shown in Figure 9, continued to precipitate after the termination of the irradiation and may be the species complexing with Am to cause the third phase during extraction.

Solutions irradiated in contact with 2 M HNO3 with air sparging were also used for Am solvent extraction experiments, with results shown in Figure 12. Although there is some scatter in the data, it appears that for aerated irradiations, there was little change in the extraction or stripping D_{Am} even at high absorbed doses. When both air-sparged and deaerated samples were irradiated in contact with an equal volume of 2 M acid, a reddish-orange oil formed at the interface (Figure 9) with increased yields with absorbed dose, and also continued to precipitate out of solution after termination of the irradiation.

4.2.4 Alpha Irradiated CMPO/dodecane Solvent Extraction Experiments

Almost no work has been done on the α-radiolysis of CMPO solutions. Only Buchholz *et al*. [6] had performed α-irradiation of CMPO-containing solutions; however, degradation yields and products were not determined in this study. Therefore, after our ^{60}Co irradiation work we investigated the α-radiolysis of this compound in dodecane under a variety of conditions, using multiple α-sources. The isotopic α-source ^{244}Cm was used to perform CMPO/dodecane irradiations at a dose rate of 1.1–1.4 kGy hour^{-1}, depending on the volume irradiated, at room temperature. These irradiations were performed in sealed 20 mL scintillation vials, with about 10 mL of headspace. The vials were opened intermittently for sampling purposes and thus these samples are considered to have been aerated throughout the irradiation. These data were compared to a He-ion beam irradiation, which was performed for sealed (deaerated) samples at a dose rate of 10.5 kGy hour^{-1}, and He/Li ion radiolysis (1.4 MeV and 0.85 MeV, respectively) on sealed samples as generated by the reaction of neutrons with ^{10}B. Different absorbed doses to these 0.1 M CMPO/dodecane samples were achieved by varying the total boron concentrations to values of 0, 0.03, 0.06, 0.09, 0.12, or 0.15 M using bis(pinacolato)diboron, to generate high-LET dose rates of 0, 43, 86, 129, 171, or 213 kGy hour^{-1}, respectively. Background corrections for gamma (estimated at ~40 kGy hour^{-1}) and neutron absorbed doses were performed by irradiating CMPO samples that contained no added boron. The temperature of the reactor-irradiated samples did not exceed 31◦C. Other details for these high LET irradiations are as described previously[25].

The effects on $-G_{CMPO}$ and the solvent extraction performance of these irradiated solutions were compared to degradation products analyses. The results for the He-ion beam irradiation of the pure organic phase containing initially 0.1 M CMPO/dodecane are shown in Figure 13. For de-aerated pure organic solution, there appears to be a slight decrease in CMPO concentration, consistent with the data shown in Figure 7. Possibly less CMPO decay is seen for irradiated, aerated, solutions. However, the minimal concentration change (due to low dose) and data error bars makes it hard to quantify this difference. Also shown in Figure 13 are data for aerated samples irradiated with the He-ion beam after pre-equilibration with 3 M HNO_3. Since acid contact reduces the apparent CMPO concentration in the HPLC-UV procedure[11] the acid-contacted sample data were normalized to an initial CMPO concentration of 100 mM. Although these acid pre-contacted data can be fitted with a line of negative slope all of the concentration values are actually within 2 σ of their mean. It was therefore concluded that the CMPO concentration remained constant for He ion beam irradiation for the acid pre-contacted conditions, again similar to the data shown in Figure 7. Lower rates of decomposition were measured for samples γ-irradiated in the presence of acid or air[20]. However, absorbed doses as high as nearly 500 kGy were employed in that work, and such trends may not be evident at the absorbed doses available with the He ion beam.

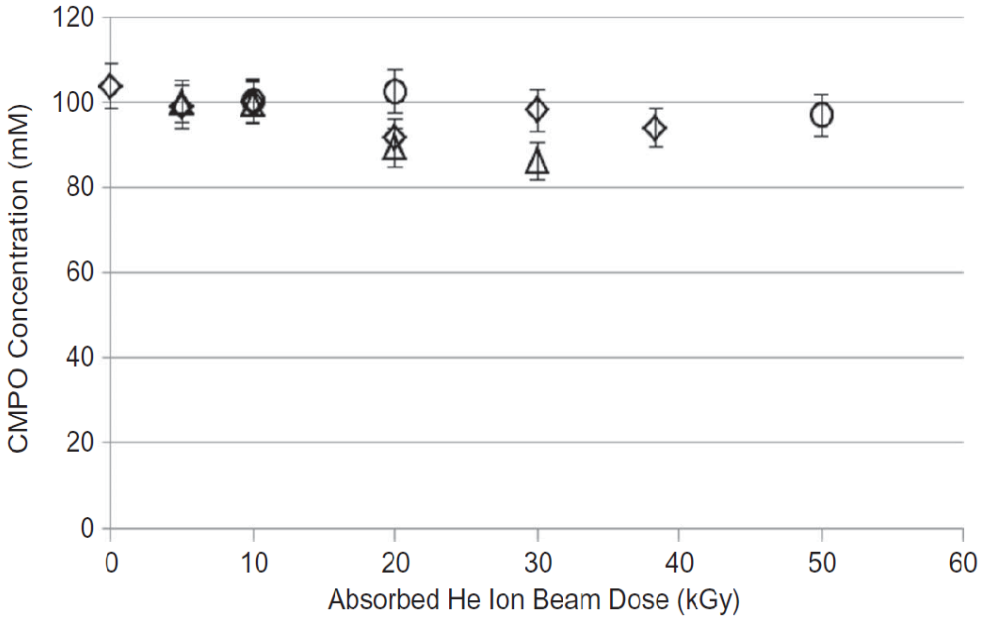

Figure 13. The change in CMPO concentration for He-ion beam irradiation of initially 0.1 M CMPO/ dodecane under various conditions. Aerated pure organic solution (diamonds), deaerated pure organic solution (circles), and aerated 3 M HNO_3 pre-equilibrated solution (triangles). The acid-equilibrated data were normalized to an initial CMPO concentration of 0.1 M. Error bars are shown for ± 5% in CMPO concentration.

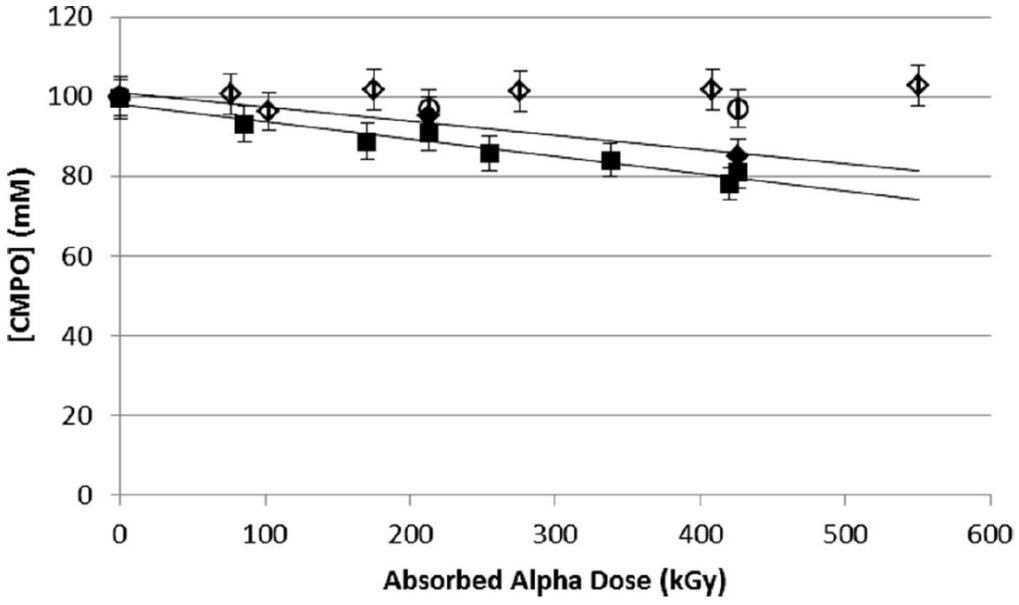

Figure 14. The change in CMPO concentration under various conditions of alpha (high LET) irradiation. ^{244}Cm irradiation in the presence of 0.1M HNO_3 (open diamonds); reactor He/Li irradiation in the presence of 0.1M HNO_3 (closed diamonds); normalized reactor He/Li irradiation in the presence of 3 M HNO_3 (open circles); and reactor He/Li irradiation with no aqueous phase (closed boxes). Error bars shown are ± 5% in CMPO concentration.

To achieve higher absorbed dose, 0.1 M CMPO/dodecane solutions were irradiated with α-radiation from the decay of ^{244}Cm. As shown in Figure 14, there was still no detectable change in CMPO concentration at the highest absorbed dose of 550 kGy, in agreement with the results found by He ion beam irradiation. Figure 14 also shows the results for reactor-generated high LET particle irradiation of 0.1 M CMPO in dodecane[9,26]. These LETs are comparable to other α-sources. For example, the LET (in water) of the particles used here range from 155.8 eV nm^{-1} for the ~5.0 MeV He ion to 213.9 eV nm^{-1} for a 1.5 MeV He ion, to 239.1 eV nm^{-1} for the 0.85 MeV Li ion[27]. This can be compared with 0.27 eV nm^{-1} or low-LET ^{60}Co γ-rays[28]. It is clear that a significant, consistent decrease in CMPO concentration occurred for samples that were reactor-irradiated in the absence of the aqueous phase, with similar results found for samples irradiated in the presence of 0.1 M HNO_3. The resulting $-G_{CMPO}$ values are 0.06 and 0.05 μmol J^{-1}, respectively, about a factor of three lower than that for γ-irradiation ($-G_{CMPO}$ ~0.18 μmol J^{-1}) under similar conditions[20]. This decrease in alpha radiolysis yield is in reasonable agreement with Camès *et al.*[30], who reported a factor-of-four lower *G*-value for DMDOHEMA radiolysis using an α-source. For samples reactor-irradiated in contact with 3 M HNO_3, no detectable loss in CMPO concentration occurred, as also shown in Figure 14, consistent with the HNO_3 radioprotection of CMPO in gamma experiments.

Americium solvent extraction experiments were performed on He-ion beam irradiated aerated, de-aerated, and 3 M HNO_3 pre-equilibrated samples. These data are shown in Figure 15. It can be seen that the distribution ratios did not change with absorbed dose, within measurement error. The presence or absence of air did not affect these values. Pre-contact with 3 M HNO_3, followed by irradiation of the wet

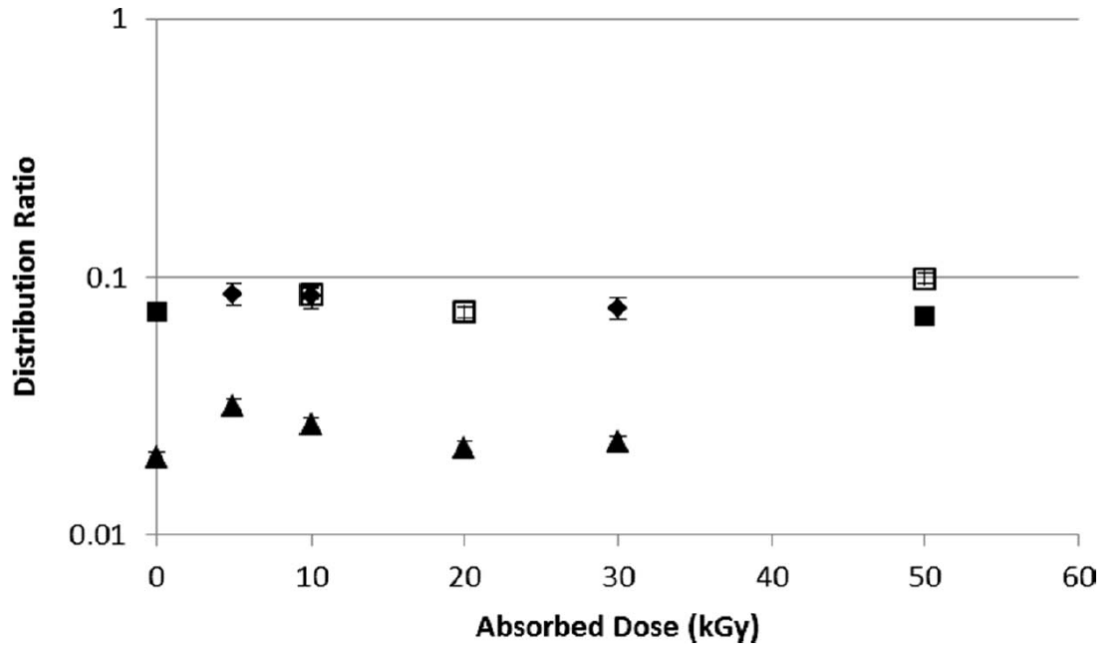

Figure 15. The solvent extraction distribution ratios of Am from 2 M HNO_3, for initially 0.1 M CMPO/ dodecane irradiated using the He-ion beam: aerated (closed diamonds); deaerated trial 1 (open boxes); deaerated trial 2 (closed boxes); pre-equilibrated with 3 M HNO_3 (closed triangles). The CMPO concentration was 0.016 M by dilution with fresh dodecane prior to extractions. Error bars are ± 10%.

organic phase, resulted in lower distribution ratios for both irradiated and non-irradiated samples. This suppression of D_{Am} was previously noted for CMPO/dodecane solutions contacted with 2 M HNO_3, where it was attributed to competition for the low ligand concentration of 0.016 M by nitric acid[20]. However, there was no downward trend in D_{Am} due to alpha irradiation. These results are in agreement with the lack of radiolytic CMPO degradation for these samples (Figures 13 and 14). The changes in extraction and stripping D_{Am} for Cm-irradiated 0.1 M CMPO/dodecane (always in contact with 0.1 M HNO_3) are shown in Figure 16. The D_{Am} values were unchanged to the highest absorbed dose for both the extraction and strip contacts, also as expected due to the lack of CMPO degradation observed for Cm-irradiated samples.

For these high LET irradiations the He-ion beam samples were analyzed by ESI-MS, as no radiological contamination of the instrument occurred for samples irradiated using this method. The main products identified[25] for non-acid equilibrated CMPO samples irradiated to 20 or 38 kGy were the amides *N,N*-diisobutylformamide (DiBFA) and *N,N*-diisobutylacetamide (DiBAA), an oxygenated derivative of DiBFA, and diisobutylamine (DiBA); these were formed by cleavage reactions on either side of the central methylene moiety of CMPO, or by cleavage of the amide bond (Figure 17).

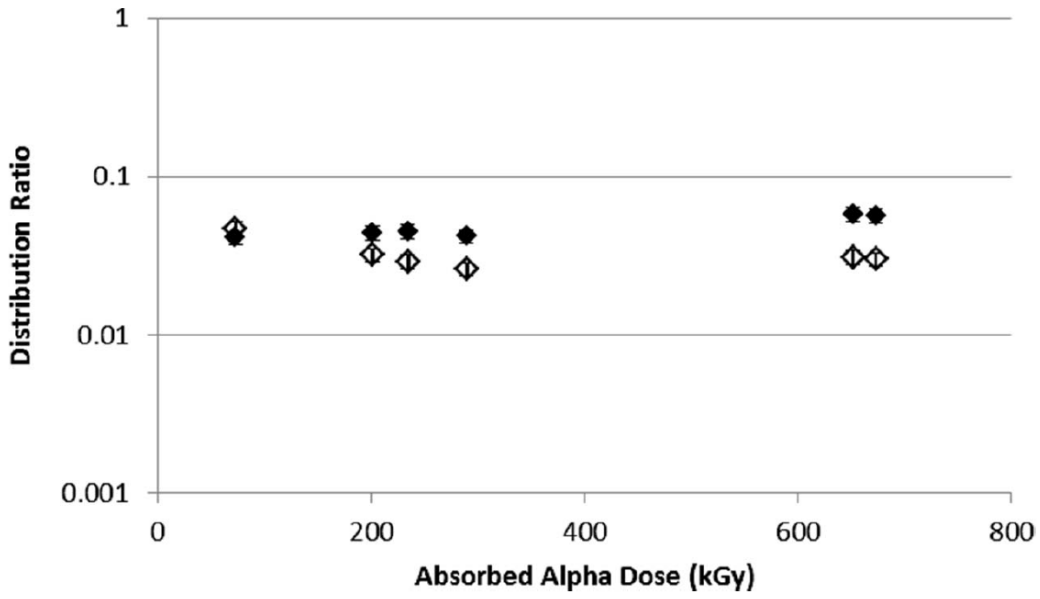

Figure 16. The solvent extraction (solid symbols) and strip distribution ratios (open symbols) of Am from 2 M HNO_3, for initially 0.1 M CMPO/dodecane irradiated using ^{244}Cm in 0.1 M HNO_3. The CMPO concentration was diluted to 0.016 M prior to extractions. Error bars shown are ± 10%.

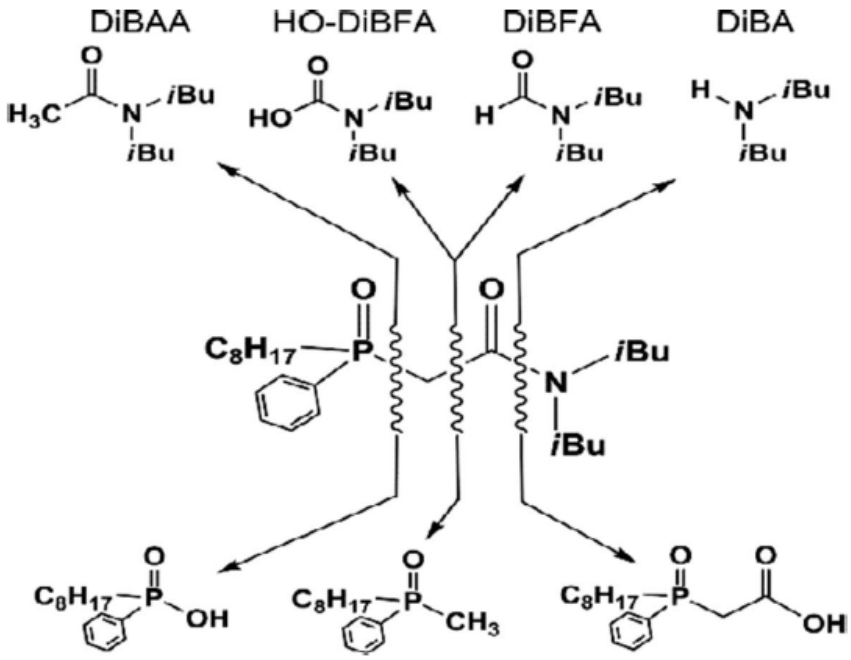

Figure 17. Cleavage pathways occurring in alpha-irradiated CMPO, as indicated by the amides DiBFA, oxy-DiBFA, DiBAA, and DiBA seen in the direct infusion ESI-MS screening of a 0.1 M CMPO/dodecane solution irradiated using a He-ion beam[25].

These cleavage reactions were accompanied by radical recombination reactions, involving mainly H• atom or HO• radical. DiBFA and oxy-DiBFA could be secondary radiolysis products of DiBAA, but in this case, cleavage exclusively at the C–P methylene bond would be indicated. Traces of DiBAA were also found in the aqueous phase when 1 mM HNO_3 was used to extract the irradiated 0.1M CMPO/dodecane, with smaller amounts of diisobutylamine (DiBA) also identified[30]. The cleavage reactions producing the amides and DiBA must also produce compounds containing the phosphoryl moiety (Figure 17). These products have been identified in the ESI-MS screening of γ-irradiation products[20,30] but were not seen in the α experiments. This indicates that they are likely present only in low concentrations (as were the amides and DiBA) and hence are difficult to measure using direct infusion ESI-MS because intact CMPO is so efficient at monopolizing charge in the ESI-MS experiment. Such low concentrations of the phosphoryl degradation products are unlikely to have a significant influence on the extraction efficiency. In their protonated form, the acetamides are water soluble, and if they act as metal complexing agents they could retain Am complexes in the aqueous phase; causing a decrease in extraction efficiency with absorbed dose. However, when we added commercially available dibutyacetamide (DBAA) over the range 0.05–1.0 mM to Am-spiked 2 M HNO_3, no change in either forward extraction or stripping D_{Am} was found.

A final comparison of the ESI-MS data for CMPO/dodecane products showed some common products. A summary of the important differences is given in Figure 18, where the major cleavages occurring are highlighted.

Figure 18. Summary of CMPO molecule cleavage for ^{60}Co (top) and alpha (bottom) radiolysis. Top: Green most probable, blue some cleavage, black minimal. Bottom: Red most probable, pink some, black minimal.

4.2.5 Radical Kinetic Experiments

As stated previously, under acidic aqueous conditions the main ligand degradation species are the hydroxyl ($HO^{\bullet}$), nitrate ($NO_3^{\bullet}$) and perhaps hydrogen atom ($H^{\bullet}$) radicals. In the organic (dodecane) phase, the chemistry is considerably simplified by the presence of dissolved oxygen, and entrained water/nitric acid. As part of this proposal, the absolute kinetics of these radicals with CMPO in dodecane were also investigated. For both high and low LET energy deposition bond scission and ionization occurs, for both the organic diluent and the entrained HNO_3. For these direct effects, the reactions occurring are[28]:

$$CH_3(CH_2)_{10}CH_3 \xrightarrow{radiation} H^{\bullet} + {}^{\bullet}CH_3 + {}^{\bullet}C_xH_y + e^-_{solv} + [CH_3(CH_2)_{10}CH_3]^{+\bullet} \quad (9)$$

$$HNO_3(org) \xrightarrow{radiation} H^{\bullet} + NO_3^{\bullet} + NO_2^{\bullet} + H^+_{solv} + O_{solv}^{\bullet-} + HNO_3^{+\bullet} + e^-_{solv} \quad (10)$$

The presence of dissolved oxygen in these aerated solutions means that all the formed solvated electrons (e_{-solv}), hydrogen atoms ($H^{\bullet}$) and carbon centered radicals ($^{\bullet}CH_3$, $^{\bullet}C_xH_y$) will quickly react to form relatively inert peroxyl radicals[17,28]. Collectively writing these species as $R^{\bullet}$, we have

$$R^{\bullet} + O_2 \rightarrow RO_2^{\bullet} \quad (11)$$

The $NO_2^{\bullet}$ radical is not reactive in either water or in alkane solution, so does not need to be further considered. The $O^{\bullet-}$ radical is highly reactive[17], and will immediately abstract a hydrogen atom off any organic species. As the diluent concentration is higher than any solute, it is expected that it will be the main reactant:

$$CH_3(CH_2)_{10}CH_3 + O_{solv}^{\bullet-} \rightarrow OH^- + CH_3(CH_2)_9C^{\bullet}HCH_3 \quad (12)$$

Both H^+_{solv} and OH^-_{solv} are non-reactive towards ligands. This leaves the dodecane radical cation $[CH_3(CH_2)_{10}CH_3]^{+\bullet}$ and the $NO_3^\bullet$ radical as the two main radical species undergoing reactions to cause ligand degradation in the organic phase. Therefore, in our study we investigated both these reactions for CMPO.

4.2.5.1 $[CH_3(CH_2)_{10}CH_3]^{+\bullet}$ Radical Cation Reactions

The electron pulse radiolysis of dodecane produces the mix of radical and ionic species listed in Equation (9). In order to isolate only the radical cation, and to quantitatively measure its reactivity with CMPO, picosecond electron pulse radiolysis/transient absorption experiments were performed at the Brookhaven LEAF facility. This facility has been described in detail previously[31]. Dodecane samples containing 0.1 – 0.5 M methylene chloride (CH_2Cl_2) were irradiated in 1.00 cm Suprasil semimicro cuvettes sealed with Teflon stoppers. The doses per pulse for various experiments were in the range 20–40 Gy. Time-resolved kinetics were obtained using a FND-100 silicon diode detector and digitized using a LeCroy WaveRunner 640Zi oscilloscope (4 GHz, 8 bit). Interference filters (~10 nm bandpass) were used for the wavelength selection of the analyzing light.

The presence of these high concentrations of CH_2Cl_2 aided the dissolved oxygen in removing solvated electrons through the reaction[17]:

$$e^-_{solv} + CH_2Cl_2 \rightarrow Cl^- + {}^\bullet CH_2Cl \qquad (13)$$

which isolates the dodecane radical cation, $[CH_3(CH_2)_{10}CH_3]^{+\bullet}$, as the only remaining reactive radical species. Initially, transient absorption spectra were obtained over the visible/near IR wavelength region, as shown in Figure 19. These spectra show that the same radical cation is initially generated under all

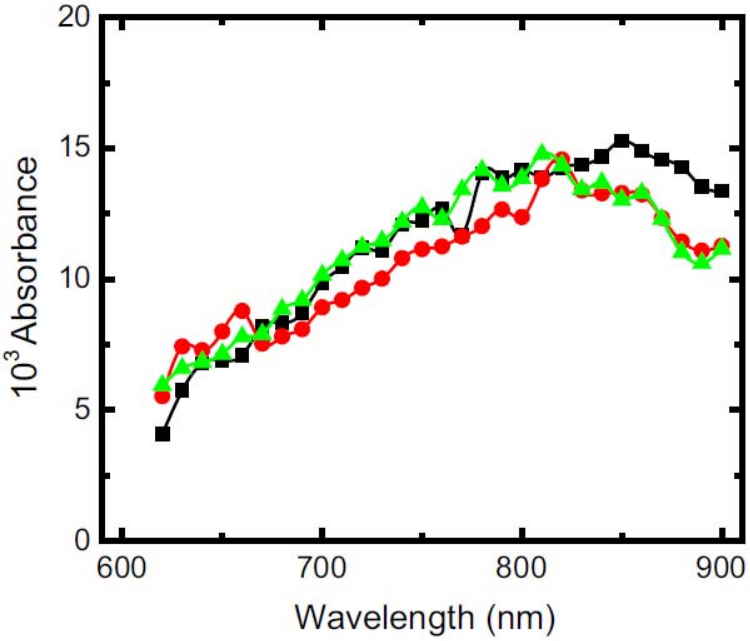

Figure 19. Dose normalized initial (t = 0, extrapolated) transient intensities for aerated dodecane (filled squares), CMPO in dodecane (filled circles) and CMPO in dodecane pre-contacted with 5 M HNO_3 (filled triangles).

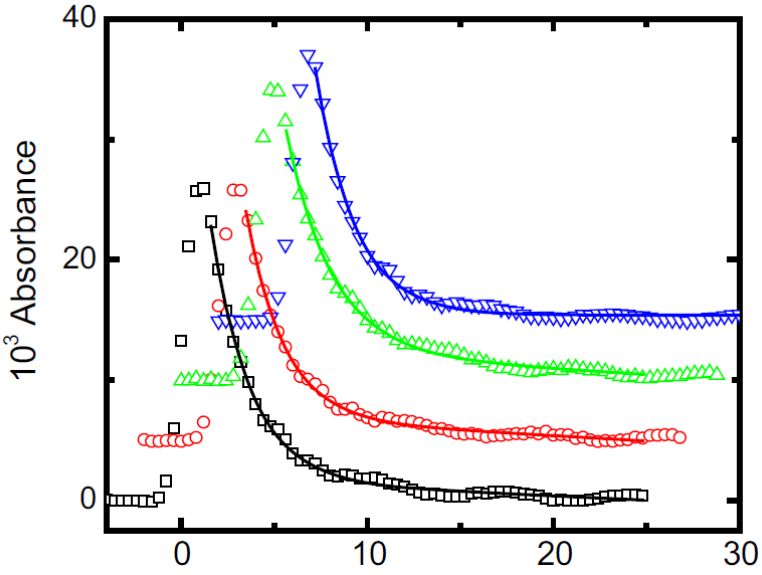

Figure 20. Transient kinetics observed[32] at 800 m nm for dodecane radical cation reaction with 5–20 mM CMPO. Data offset in both time and absorbance intensity to aid clarity. Solid lines are exponential decay fits, with corresponding first-order rate constants of (5.05 ± 0.27) x 10^8 (open square, 5 mM CMPO), (5.48 ± 0.34) x 10^8 (open circle, 10 mM CMPO), (6.01 ± 0.66) x 10^8 (open triangle, 15 mM CMPO), and (6.85 ± 0.52) x 10^8 (open down triangle, 20 mM CMPO) s^{-1}, respectively.

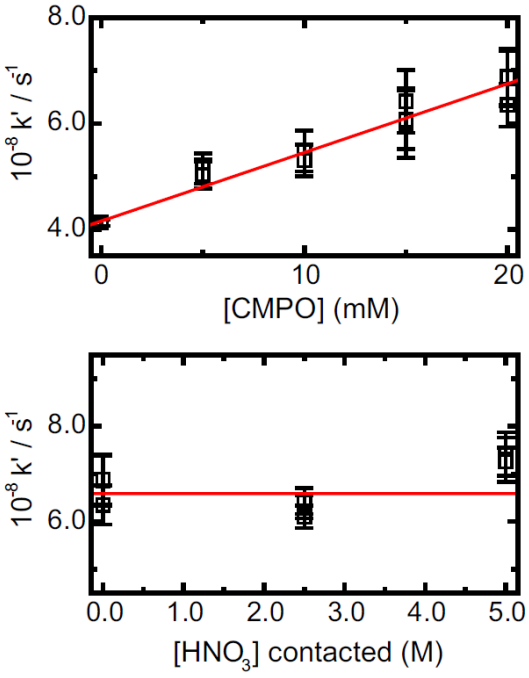

Figure 21. Top: Second-order rate constant plot for reaction of dodecane radical cation ($R^{+\bullet}$) with CMPO in dodecane/0.10 M CH_2Cl_2 at 295 K. Individual data points and corresponding error bars are the average of 3 individual measurements for each concentration of CMPO. Solid line is weighted linear fit, corresponding to a slope of k_8 = (1.30 ± 0.11) x 10^{10} M^{-1} s^{-1}, (R^2 = 0.96). Bottom: Measured rate constants for 20 mM CMPO in aerated dodecane/0.10 M CH_2Cl_2 contacted with different nitric acid concentrations showing no significant increase in reactivity.

conditions, and that the cation is apparently not immediately quenched by nitric acid contact. However, the kinetics of the dodecane radical cation at 800 nm are seen to decay faster in the presence of increasing amounts of CMPO (Figure 20)[32]. These individual decays were fitted to an exponential decay function, which also included a small baseline adjustment. The pseudo-first-order rate constants obtained were plotted against the CMPO concentration, see Figure 21, top, whose slope gave a second-order rate constant for the reaction:

$$[CH_3(CH_2)_{10}CH_3]^{+\bullet} + [CMPO_x\bullet(HNO_3)_y] \rightarrow CH_3(CH_2)_{10}CH_3 + [CMPO_x\bullet(HNO_3)_y]^{\bullet} / \text{products} \quad (14)$$

This was the first ever measured rate constant for the dodecane radical cation with this ligand.

This rate constant is nearly diffusion-controlled, indicating that the reaction of the dodecane radical cation could be a major concern under process conditions. In addition, this value can be compared to the previous finding that the rates of CMPO degradation in gamma-irradiations under similar solution conditions, where it was observed that pre-contact of nitric acid provided a protecting effect of CMPO degradation[20]. The decreased CMPO degradation rate ($-G_{CMPO}$) was attributed to the protective effect of the formation of a $[CMPO_x\bullet(HNO_3)_{y+1}]$ complex in dodecane:

$$[CMPO_x\bullet(HNO_3)_y]\,(org) + HNO_3(aq) \leftrightharpoons [CMPO_x\bullet(HNO_3)_{y+1}](org) \qquad K_7 = 0.15 \pm 0.01 \quad (7)$$

As such, equivalent kinetic measurements were made for the highest concentration of 20 mM CMPO with two acid pre-contacts, 2.5 M and 5.0 M HNO_3.[33] These kinetic data are shown in Figure 21, bottom. No significant change in the chemical reaction reactivity was observed. This constant behavior at the different acid concentration contacts remains consistent with the interpretation that the charge transfer still occurs at effectively a diffusion controlled rate with the formed nitric acid complex:

$$[CH_3(CH_2)_{10}CH_3]^{+\bullet} + [CMPO_x\bullet(HNO_3)_{y+1}] \rightarrow CH_3(CH_2)_{10}CH_3 + [CMPO_x\bullet(HNO_3)_y] + [HNO_3]^{+\bullet} \quad (15)$$

However, for the $-G_{CMPO}$ data previously reported to be consistent with the measured kinetics, the charge transfer reaction that occurs with the nitric acid complex would have to have to regenerate free unchanged $[CMPO_x\bullet(HNO_3)_y]$ (Reaction 15) whereas the charge transfer with the $[CMPO_x\bullet(HNO_3)_y]$ or dry CMPO would have to directly result in ligand degradation (Reaction 14). This chemistry is still under investigation, with different ligands and diluents being studied to provide further insight into these radical cation reactions.

4.2.5.2 $NO_3^{\bullet}$ Radical Reactions in Organic Solvents

As detailed above, there are multiple routes by which the $^{\bullet}NO_3$ radical can be formed in the organic solvent system, and therefore, we also investigated this chemistry in this work. Unfortunately, no suitable source of the $^{\bullet}NO_3$ radical in dodecane was found over the course of this study. Experimentation showed that the chemical tetrabutylammonium nitrate ($(C_4H_9)_4NNO_3$) was sufficiently soluble in lower molecular weight alcohols, particularly *tert*-butanol (~1.25 M) to allow direct irradiation effects to produce small but useable amounts of the nitrate radical. However, this compound was barely soluble in dodecane, and its radiolysis did not give any useful transient absorbance. The use of the tetraoctylammonium nitrate analogue was also insufficiently soluble, and even synthesis and use of the tetradodecylammonium nitrate salt was not successful. Lastly we tried using amyl nitrate, but while soluble in dodecane, its radiolysis resulted in the nitrite ($^{\bullet}NO_2$) radical rather than $^{\bullet}NO_3$. At this time we are still searching for a suitable source molecule to allow us to generate $^{\bullet}NO_3$ radicals in dodecane.

However, as a benchmark reference, multiple experiments were conducted using tetrabutyl-ammonium nitrate in *tert*-butanol. The radiolysis of a saturated solution of this compound using relatively high doses (~20 Gy) gave the transient absorption spectrum shown in Figure 22. This spectrum is identical to that generated in aqueous solution using 6.0 M HNO_3, but red-shifted by 10-20 nm. The decay of this transient species was found to be first order, and faster when a solute such as CMPO was added

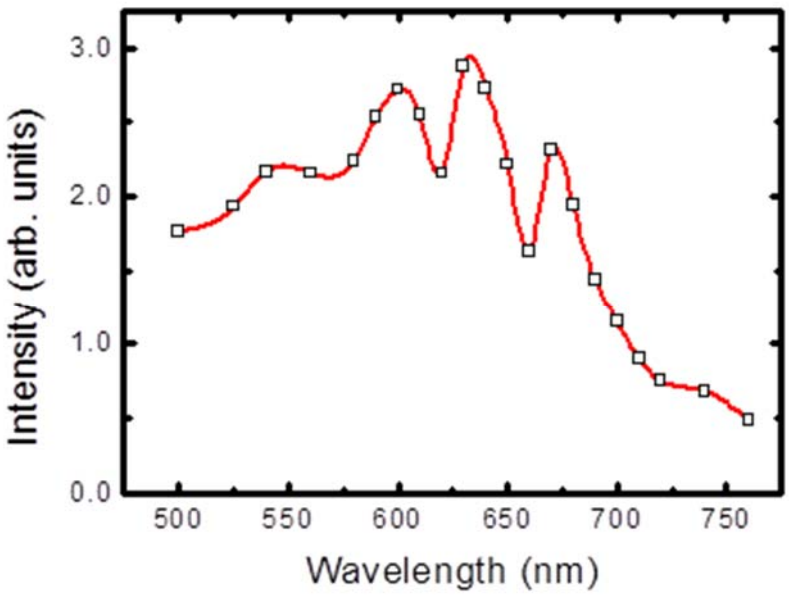

Figure 22. Initial (zero-time, extrapolated) UV-visible absorption spectrum of the $^{\bullet}NO_3$ radical in *tert*-butanol generated through direct radiolysis of 1.25 M $(C_4H_9)_4NNO_3$ dissolved in dodecane at 22°C.

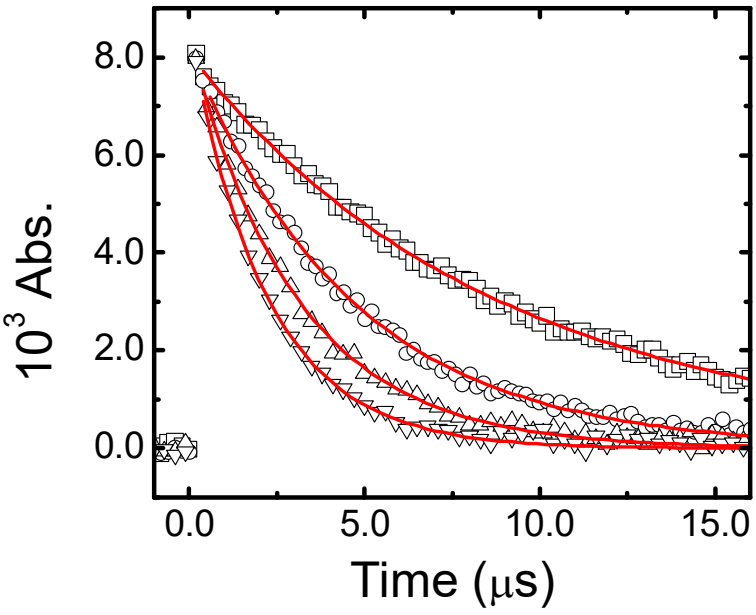

Figure 23. Pseudo-first-order kinetic decays observed for $^{\bullet}NO_3$ radical in tert-butanol with added CMPO; 22 μM (□), 63 μM (O), 80 μM (Δ) and 100 μM(∇). Solid lines are fitted exponential decays, giving the rate constants plotted in Figure 24.

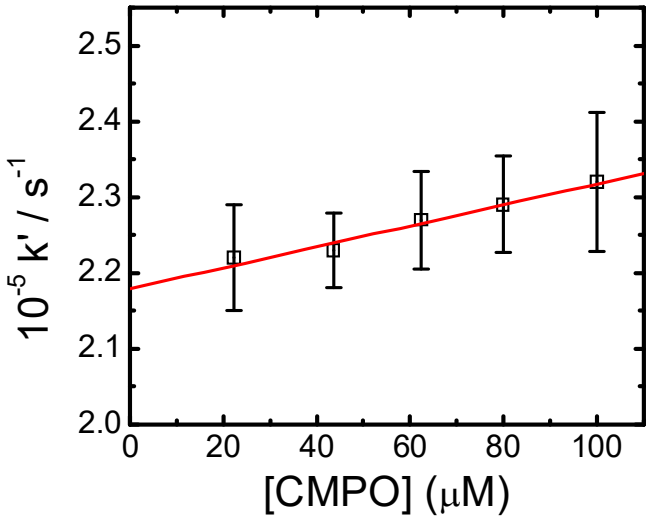

Figure 24. Second-order rate constant determination for the reaction of the $^{\bullet}NO_3$ radical with CMPO in dodecane. Error bars are one standard deviation as obtained from 3-4 individual measurements. Solid line is weighted linear fit, corresponding to second-order rate constant of $k_{16} = (1.28 \pm 0.13) \times 10^8$ M^{-1} s^{-1}.

(see Figure 23). By fitting pseudo-first-order decay kinetics to these observed traces, and then plotting the fitted first-order rate constants against the CMPO concentration (Figure 24) the absolute, second-order rate constant k_{16} for the reaction of

$$^{\bullet}NO_3(org) + CMPO(org) \rightarrow products \qquad k_{16} = (1.28 \pm 0.13) \times 10^8\ M^{-1}\ s^{-1} \qquad (16)$$

was obtained. This rate constant is slightly faster than determined in aqueous solution (see next section).

4.3 Ligand kinetic studies

4.3.1 Hydroxyl radical reactions with DTPA

One significant portion of this work was the measurement of aqueous radical kinetics with various ligands anticipated for use in large-scale solvent extraction based nuclear fuel reprocessing. As shown previously, the important radicals are the hydroxyl radical ($HO^{\bullet}$), nitrate radical ($^{\bullet}NO_3$) and under certain circumstances, hydrogen atom ($H^{\bullet}$). The following section is a short summary of how these measurements were performed, utilizing the Linear Accelerator facilities at the Radiation Research Laboratory, University of Notre Dame, and the rate constants for various ligands measured.

For $HO^{\bullet}$ radical chemistry the ligand DTPA (diethylenetriaminepentaacetic acid) was chosen for detailed study. As the reaction of $HO^{\bullet}$ with DTPA did not produce any significant UV-visible transient absorbance over the range 250 – 800 nm, these kinetics were measured using SCN^- competition kinetics. This approach is based on using KSCN as a standard[17], and competing the $HO^{\bullet}$ radical against it by addition of the DTPA. The reactions corresponding to this chemistry at 22°C and neutral pH are:

$$HO^{\bullet} + SCN^- (+ SCN^-) \rightarrow OH^- + (SCN)_2^- \qquad k_{17} = 1.05 \times 10^{10}\ M^{-1}\ s^{-1} \qquad (17)$$

$$HO^{\bullet} + DTPA \rightarrow products \qquad k \qquad k_{18} \qquad (18)$$

These kinetics are just a coupled differential equation, which can be readily solved to give the analytical expression:

$$\frac{Abs^{o}(SCN)_2^{-*}}{Abs(SCN)_2^{-*}} = 1 + \frac{k_{18}[DTPA]}{k_{17}[SCN^-]} \qquad (19)$$

where $Abs^{\circ}(SCN)_2^{-\bullet}$ is the total absorbance measured from the yield of $(SCN)_2^{-\bullet}$ in a solution of only SCN^- (blank), while $Abs(SCN)_2^{-\bullet}$ is the absorbance measured for $(SCN)_2^{-\bullet}$ with DTPA present. By plotting the absorbance ratio $Abs^{\circ}(SCN)_2^{\bullet-}$/ $Abs^{\circ}(SCN)_2^{\bullet-}$ versus [DTPA]/[SCN^-] a straight line is observed with a y-intercept of 1.0 and a slope of k_{18}/k_{17}. From the known k_{17} value, the k_{18} rate constant is determined.

Typical data for these kinetics and transformed plot are shown in Figure 25. From the transformed linear plot (Figure 25, bottom) a reaction rate constant of $k_{18} = (2.28 \pm 0.07) \times 10^9$ M^{-1} s^{-1} is obtained for these conditions. DTPA has a number of protonated species, which are pH dependent[34]. For example, at the TALSPEAK system pH of 3.6 there are significant amounts of four different protonated DTPA species. Therefore, it was important to determine the rate constants for the reaction of the hydroxyl radical with each of these species. Based on the speciation diagram, generated using known pKa values[34] (see Figure 26) fractional components of each DTPA species could be calculated under any pH and temperature condition. In this study we assumed that the overall rate constants obtained at both pH 1.0 and pH 6.0 were assumed to be equal to the rate constants for the H_5-DTPA and H_2-$DTPA^{3-}$ species respectively. This assumption was based on the fact that the percentage of these species at those pH's was 98% or higher. Intermediate pH rate constants was the weighted sum of the individual species' rate constants, according to:.

$$k_{overall} = \alpha_{DTPA\text{-}H5} \times k_{DTPA\text{-}H5} + \alpha_{DTPA\text{-}H4} \times k_{DTPA\text{-}H4} + \alpha_{DTPA\text{-}H3} \times k_{DTPA\text{-}H3} + \alpha_{DTPA\text{-}H2} \times k_{DTPA\text{-}H2} \qquad (20)$$

with a being the fractional contribution of each protonated species and k the corresponding rate constant for that species. It is important to note that although there are several other pKa values for more acidic pH's these were assumed to be similar to those obtained at pH 1.

The measured reaction rate constants at various temperatures and pH's are summarized in Table 1. Combining these with the temperature-dependent pKa values and plots as shown in Figure 26, individual rate constants for H_4-$DTPA^-$ and H_3-$DTPA^{2-}$ were calculated. The resulting rate constants are shown in Table 2. The rate constants for H_3-DTPA, H_4-DTPA, and H_5-DTPA are all very similar at the same temperature, while the rate constant of H_2-$DTPA^{3-}$ is significantly larger. The similarity of the reaction rate constants for the H_3-, H_4-, and H_5-DTPA validates our assumption that the more protonated species at much higher acidities (lower than pH 1) would be the very similar to that of H_5-DTPA.

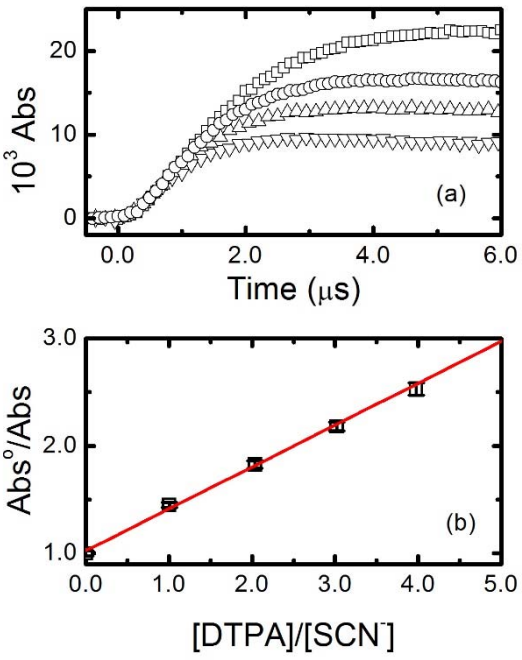

Figure 25. Top: Transient absorbance of $(SCN)_2^-$ from N_2O-saturated 102.4 μM KSCN solution containing zero (□), 102.8 (O), 208.5 (Δ), and 406.9 (∇) □M DTPA at pH 6.00 and 23.8°C. Bottom: Competition kinetics plot for the determination of second order rate constant of hydroxyl radical using ratios of limiting absorbance of kinetic traces of top. Solid line is weighted linear fit, with slope of m = (2.69 ± 0.07) x 10^{-1}, intercept of I = 0.999 ± 0.009, R^2 = 0.998. This slope corresponds to k_{18} = (2.28 ± 0.07) x 10^9 M^{-1} s^{-1}.

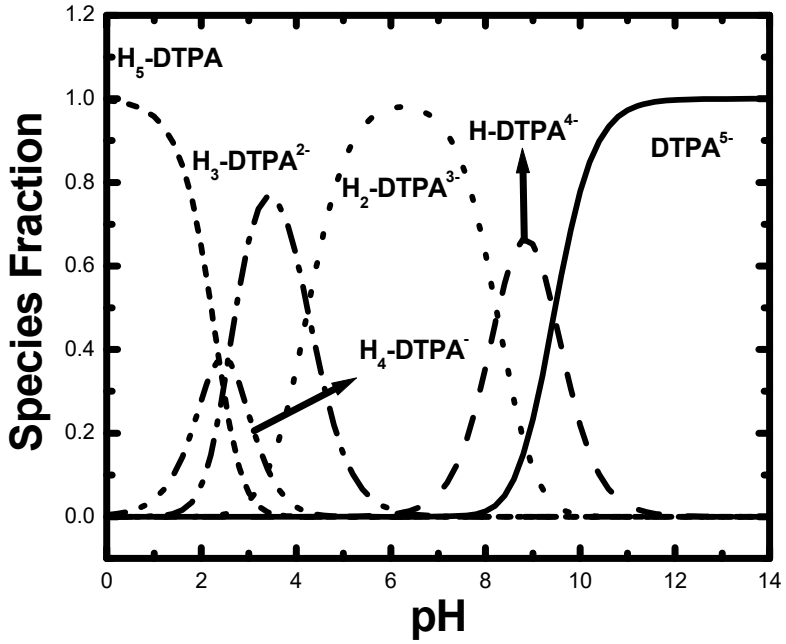

Figure 26. Fractionation plot for the protonated species of DTPA at 25˚C generated using literature pKa values.

Table 1: Overall measured rate constants determined for hydroxyl radical reaction with DTPA.

pH	Temp. (K)	10^{-9} k ($M^{-1}s^{-1}$)	1/T (K^{-1})	ln (k)
1.0	281.53	2.19	0.00353	21.508
1.0	288.81	2.50	0.00346	21.640
1.0	294.83	2.82	0.00339	21.760
1.0	301.87	3.29	0.00320	21.914
1.0	311.54	3.95	0.00321	22.096
2.0	283.03	2.11	0.00353	21.469
2.0	288.73	2.40	0.00346	21.598
2.0	294.83	2.71	0.00339	21.720
2.0	312.50	3.69	0.00320	22.030
4.3	282.23	2.33	0.00354	21.569
4.3	292.29	3.20	0.00342	21.886
4.3	302.70	4.17	0.00330	22.151
4.3	310.91	5.11	0.00322	22.354
6.0	282.49	3.06	0.00354	21.841
6.0	292.36	4.03	0.00342	22.116
6.0	302.70	5.29	0.00330	22.389
6.0	310.91	7.13	0.00322	22.688

Table 2: Temperature-dependent rate constants determined for different DTPA species

DTPA Species	Temp. (K)	10^{-9} k ($M^{-1}s^{-1}$)	1/T (K^{-1})	ln (k)
H_2-DTPA^{3-}	282.49	3.06	0.00354	21.841
	292.36	4.03	0.00342	22.116
	302.70	5.29	0.00330	22.389
	310.91	7.13	0.00322	22.688
H_3-DTPA^{2-}	282.23	1.83	0.00354	21.326
	292.29	2.35	0.00342	21.577
	302.70	2.66	0.00330	21.703
	310.91	2.98	0.00322	21.814
H_4-DTPA^{-}	283.03	2.11	0.00353	21.469
	288.73	2.13	0.00346	21.479
	294.83	2.42	0.00339	21.607
	312.50	3.09	0.00320	21.852
H_5-DTPA	281.53	2.19	0.00353	21.508
	288.81	2.50	0.00346	21.640
	294.83	2.82	0.00339	21.760
	301.87	3.29	0.00320	21.914
	311.54	3.95	0.00321	22.096

Table 3: Thermodynamic parameters determined for the different DTPA species.

DTPA Species	E_a (kJ mol^{-1})	$\Delta H^{\ddagger}$ (kJ mol^{-1})	$\Delta S^{\ddagger}$ (J mol^{-1} K^{-1})
H_2-DTPA^{3-}	21.37 ± 1.39	18.91 ± 1.37	3.93 ± 4.62
H_3-DTPA^{2-}	12.11 ± 1.32	9.65 ± 1.34	-32.73 ± 4.51
H_4-DTPA^{-}	13.39 ± 1.68	7.69 ± 1.27	-39.10 ± 4.33
H_5-DTPA	14.45 ± 0.41	11.99 ± 0.40	-23.13 ± 1.34

In order to determine the thermodynamic parameters of these reactions, the Arrhenius and the Eyring equations were used. These equations allowed for the determination of the enthalpy ($\Delta H^{\ddagger}$), and entropy ($\Delta S^{\ddagger}$) of activation, as well as the activation energy (E_a) and the pre-exponential factor (A). These data are summarized in Table 3. Again it is seen that the only species that is significantly different is H_2DTPA^{3-}, which has a significantly higher activation energy (E_a), enthalpy of activation ($\Delta H^{\ddagger}$) and the only positive entropy of activation ($\Delta S^{\ddagger}$) value.

4.3.2 Hydroxyl radical reaction with metal-loaded ligands

Under anticipated large-scale process conditions considerable fractions of the ligand will be bound to metal ions. For TALSPEAK, DTPA acts as a hold-back agent, complexing actinides to prevent them from being extracted into the organic phase. As such, considerable effort in this project was spent elucidating reaction rate constants for the important radicals with metal-loaded ligands. For the hydroxyl radical the same approach was used for metal(M)-DTPA(L) complexes, based upon SCN^- competition kinetics[17]. Separate experiments confirmed that the lanthanide ions themselves did not oxidize by reaction of $HO^{\bullet}$ radicals, therefore, experiments were conducted using a slightly limiting amount of DTPA. It was always assumed that a 1:1 complex was always formed, so M:L ratios of 1:1.1-1.2 were always used in aqueous solution.

Typical data are shown in Figure 27 for Eu-DTPA. The rate constant under these conditions was determined to be $k = (3.63 \pm 0.04) \times 10^9$ M^{-1} s^{-1}, substantially faster than determined for free DTPA alone. Following this methodology for a series of lanthanide-DTPA complexes, the rate constants summarized in Table 4 were obtained. These data are shown graphically in comparison to free DTPA in Figure 28. It is seen that at pH 2, a significant decrease in $HO^{\bullet}$ reactivity occurs, whereas at higher pH's, the reactivity remains constant. This is in contrast to free DTPA that shows an increasing reactivity over the pH 2-6 range. We attribute this change in reactivity in the metal-loaded system to the protonation of the active reaction site at the lower pH's. This is not evident in the reaction rate constants observed for free DTPA, indicating that the metal complexation impacts the chemistry of the DTPA significantly. Based on literature comparison and complexation of DTPA with other metals, this site is probably one of the constituent nitrogen atoms becoming further protonated, which would reduce its reactivity.

Presently, we are investigating other $HO^{\bullet}$ reactions with lanthanides bonded to different ligands, as well as temperature effects to obtain Arrhenius and thermodynamic parameters.

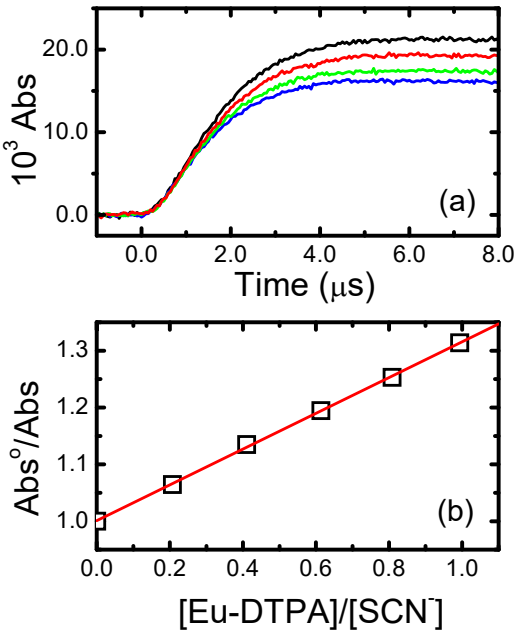

Figure 27. a) Measured $(SCN)_2^{-\bullet}$ absorbance for N_2O-saturated, 100.3 μM KSCN and 199.6 μM Eu^{3+} with zero (top black), 20.8 (red), 61.6 (green) and 99.7 (bottom blue) μM DTPA at pH 3.03 and 21.9ºC. b) Transformed competition kinetics plots for Eu-DTPA at from peak absorbance data of a). Solid line corresponds to linear fits, from which are determined specific rate constants for hydroxyl radical reaction with Eu-DTPA of k = (3.63 ± 0.04) x 10^9 M^{-1} s^{-1}.

Table 4. Summary of Lanthanide-DTPA and hydroxyl radical reaction rate constants.

Metal ion	pH	Temp ºC	10^{-9} k M^{-1} s^{-1}	Metal ion	pH	Temp ºC	10^{-9} k M^{-1} s^{-1}
Lu^{3+}	22	22.1	2.98 ± 0.27	Eu^{3+}	2	19.4	2.95 ± 0.04
	3	21.8	3.42 ± 0.03		3	21.9	3.63 ± 0.04
	3.6	23.3	3.30 ± 0.12		4	22.2	3.55 ± 0.02
	5	21.0	3.23 ± 0.11		5	21.4	3.56 ± 0.17
Er^{3+}	2	22.2	3.27 ± 0.05	Nd^{3+}	2	22.2	3.51 ± 0.12
	3	22.6	3.84 ± 0.09		3.6	22.6	3.49 ± 0.13
	3.6	22.2	3.89 ± 0.07		5	22.3	4.15 ± 0.47
	5	21.9	3.91 ± 0.12	La^{3+}	2	21.5	2.84 ± 0.06
Gd^{3+}	2	22.1	3.64 ± 0.06		3.6	21.4	3.12 ± 0.16
	3	21.8	4.80 ± 0.09		5	22.1	3.61 ± 0.26
	3.6	20.6	4.23 ± 0.10				
	5	20.8	4.42 ± 0.05				

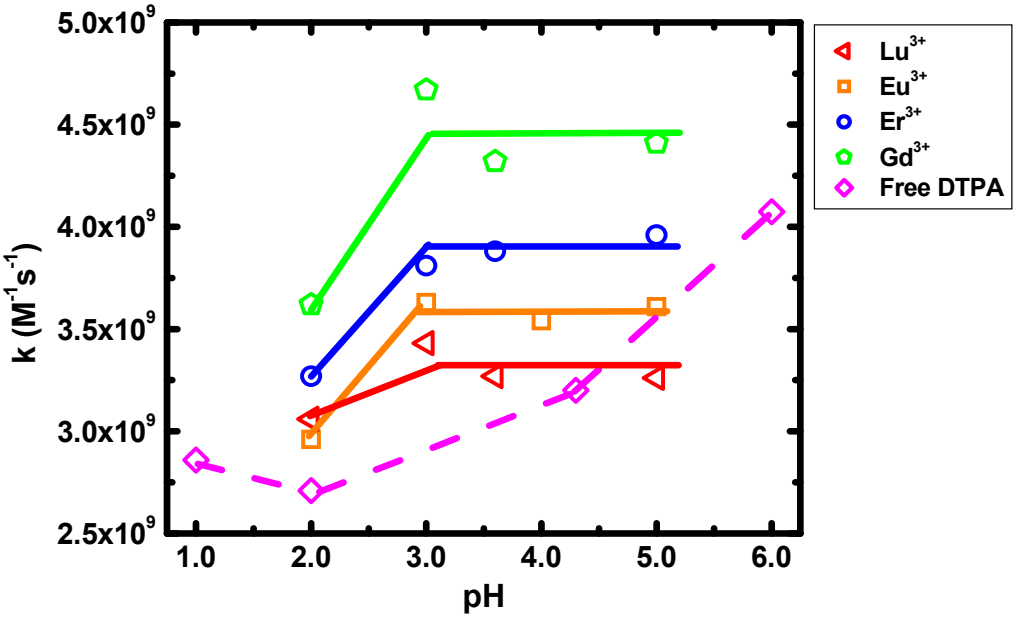

Figure 28. Summary of pH-dependent hydroxyl radical rate constants with metal-loaded DTPA at room temperature (20-22°C). Also shown are the equivalent data for free DTPA ligand in aqueous solution.

4.3.3 Nitrate radical reaction with free and metal-loaded ligands

As detailed for the organic (*tert*-butanol) experiments, the $NO_3^\bullet$ radical was readily generated using direct radiolysis effects on 6.0 M HNO_3 solutions. The same transient absorption spectrum, blue-shifted by 10-20 nm, was obtained, see Figures 22. Absolute kinetics were obtained in the same way as in *tert*-butanol, typical examples are shown in Figures 29 and 30 for the modifier Cs-7SB. A number of ligands, and other species relevant to the nuclear fuel reprocessing industry were studied in this portion of the project. A summary of the rate constants obtained is given in Tables 5. These aqueous values were compared to organic media wherever possible. It was generally seen that the $NO_3^\bullet$ radical reacted slightly faster in organic (*tert*-butanol) solution than in aqueous solution. Mechanistically, it is expected that similar reactions occurred; with $NO_3^\bullet$ radical addition to aromatic rings. These reactions occurred much faster for methyl-substituted phenyl rings, where electron abstraction from the terminal methyl moiety allows formation of the semi-stable aromatic 7-membered tropylium cation. Nitration of the aromatic rings though significantly reduced additional $NO_3^\bullet$ reactivity. Lastly, just as for the hydroxyl radical, much faster (almost an order-of-magnitude) rate constants were obtained for metal-ligand complexes in the organic phase (1:3 complexes, with a slight excess of non-reactive metal ions) than for the free ligand alone.

In an attempt to understand $NO_3^\bullet$ reaction mechanisms in general, significant work was performed on rate constant determination for multiple species in *tert*-butanol and 6.0 M HNO_3 solution. An excellent linear correlation was obtained between these two diluents, as shown in Figure 31. Effort is currently on-going to expand this dataset.

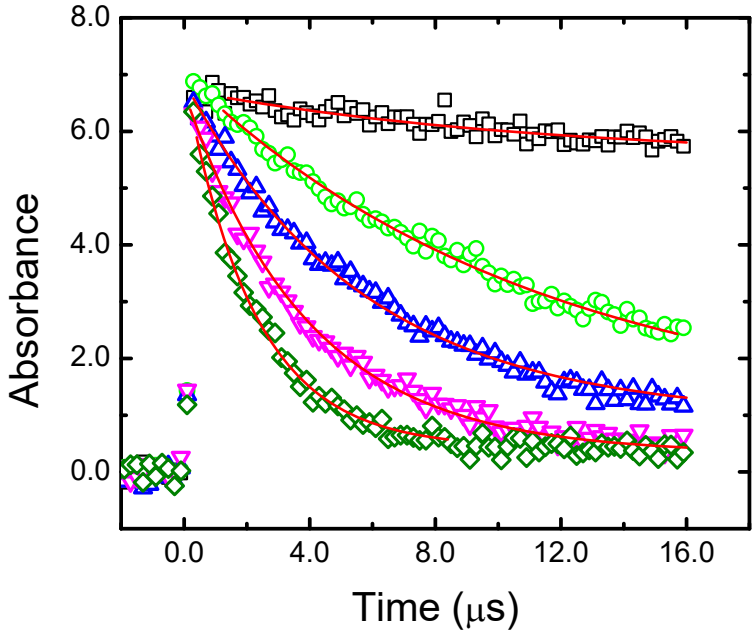

Figure 29. Typical first-order decay kinetic data obtained at 630 nm for $NO_3^\bullet$ radical reaction with Cs-7SB in 6.0 M HNO_3 at 22.2ºC.

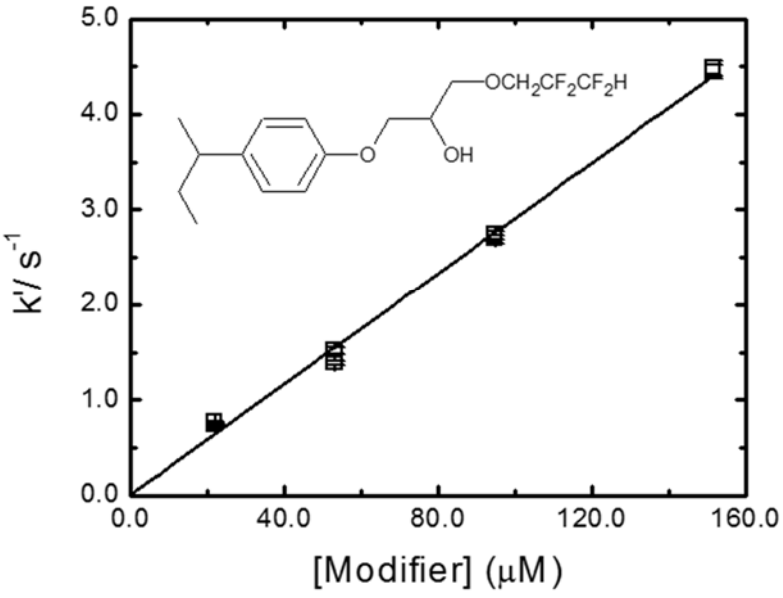

Figure 30. Second order-determination of reaction rate constant for $NO_3^\bullet$ radical reaction with Cs-7SB in 6.0 M HNO_3 at 22.2ºC. Slope of line gives k = (2.90 ± 0.03) x 10^9 M^{-1} s^{-1}. Inset is structure of Cs-7SB modifier.

Table 5. Summary of measured $NO_3^{\bullet}$ radical rate constants obtained for ligands and other species of relevance to the nuclear fuel reprocessing industry.

Analyte	Organic Phase (tert-butanol) $k / M^{-1} s^{-1}$	Aqueous phase (6.0 M HNO_3) $k / M^{-1} s^{-1}$
TBP	$(1.42 \pm 0.09) \times 10^7$	$(4.3 \pm 0.7) \times 10^6$
CMPO	$(3.24 \pm 0.17) \times 10^8$	$(1.28 \pm 0.13) \times 10^8$
DMDOHEMA	$(4.27 \pm 0.46) \times 10^8$	$(2.22 \pm 0.10) \times 10^8$
CMPO•Nd	$(3.37 \pm 0.05) \times 10^9$	
CMPO•Eu	$(2.52 \pm 0.05) \times 10^9$	
Cs7SB		$(2.90 \pm 0.03) \times 10^9$
Benzene		$< 1 \times 10^6$
Toluene		$(1.71 \pm 0.06) \times 10^9$
3-nitrotoluene		$(2.80 \pm 0.05) \times 10^7$
2,4-dinitrotoluene		$(3.07 \pm 1.45) \times 10^5$

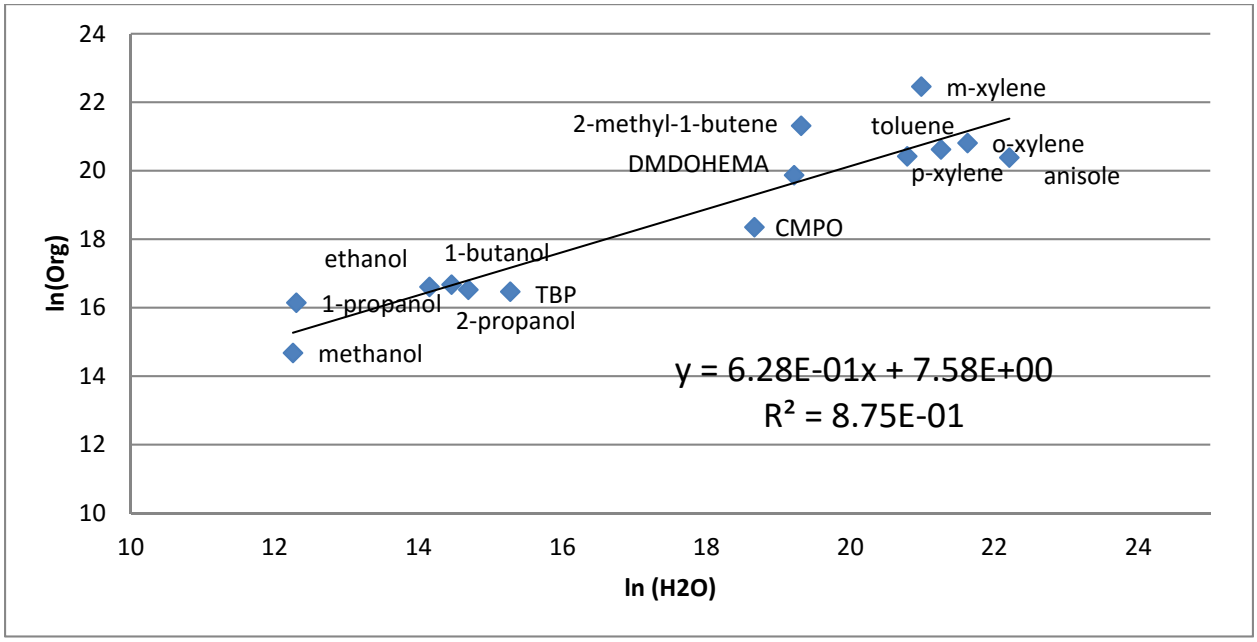

Figure 31. Correlation plot of $\ln(k_{org}/M^{-1} s^{-1})$ against $\ln (k_{H2O}/M^{-1} s^{-1})$ for various chemical species. Equation given is non-weighted linear fit. R^2 value shows excellence of correlation.

4.4 TBP irradiation studies

The stability of TBP in organic media has been the basis of the PUREX extraction system for many years, however, little high LET work has been done. The main efforts for investigating the degradation of this ligand were undertaken using the TRIGA™ reactor irradiation facility at the University of California, Irvine, California. The advantage to this system was that large doses (hundreds of kGy) were obtainable quickly, and that the mixed gamma/alpha radiolysis field was representative of the conditions anticipated under real-world, large-scale reprocessing conditions. However, the mixed field irradiation meant that deconvolution of the individual gamma and alpha effects needed to be performed utilizing computer programs. Moreover, the method of alpha generation, through the $^{10}B(n,\alpha)^{7}Li$ reaction (see Figure 2) gave two high LET particles that were significantly different in energy than the isotope alpha decay; the total energy of ~2.79 MeV is partitioned by the alpha particle (~1.47 MeV) and the ^{7}Li recoil (~0.84 MeV)[10]. Although one can assume these are similar enough to be equivalent to only alpha irradiation, this gives a slightly different yield of radical species, as shown in Figure 32 for the standard Fricke dosimeter.

Initial attempts utilizing the TRIGA™ reactor were focused upon obtaining reliable dosimetry for irradiations performed in dodecane[35]. From a combination of the dye methyl red as compared to the standard Fricke dosimeter (see Figure 32) absolute dose deposition for mixed field gamma and alpha irradiation was obtained. The advantage of using the methyl red system was that it could also be used in separate gamma-irradiation (^{137}Cs) experiments, allowing deconvolution of the mixed irradiation field data to be more readily performed. These data are shown in Figures 33 and 34. Computer modeling and deconvolution of this irradiation system was also performed for the experimental data, excellent agreement is consistently seen. The α radiolysis based degradation is about an order of magnitude less than for γ.

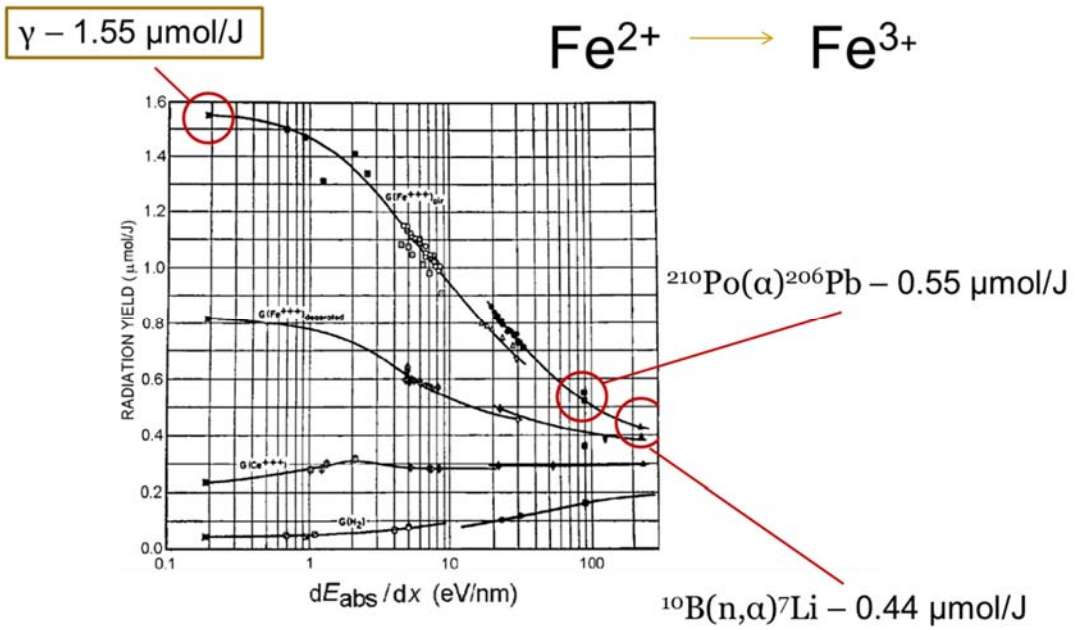

Figure 32. Radiation chemistry of the Fricke dosimeter for various LET ($\Delta E_{abs}/dx$) species[28]. Circled values are comparison of high LET α He^{2+} vs the $^{10}B(n,\alpha)^{7}Li$ generated species.

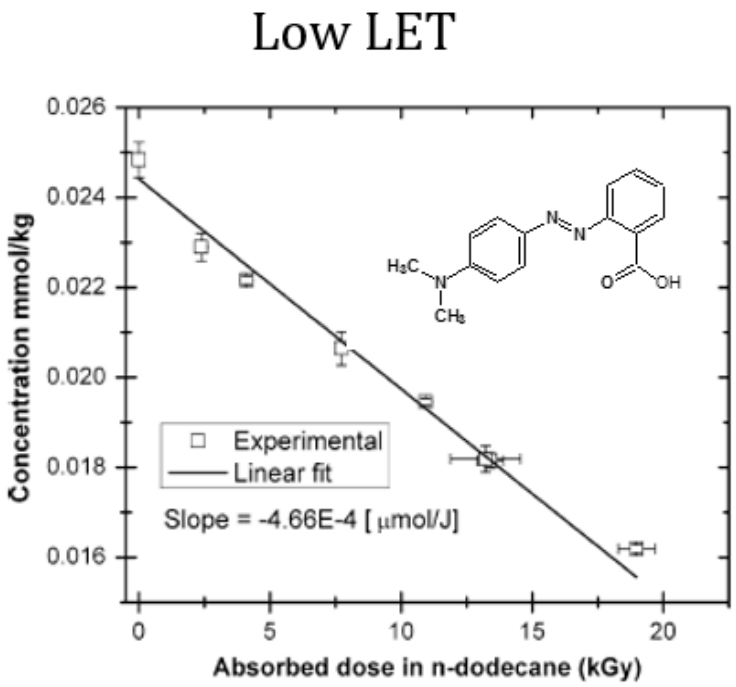

Figure 33. Low LET (^{137}Cs) γ irradiation of methyl red (structure inset) in dodecane. Solid line is computer model fit. Degradation efficiency is 4.68 x 10^{-4} μmol J^{-1} at room temperature.

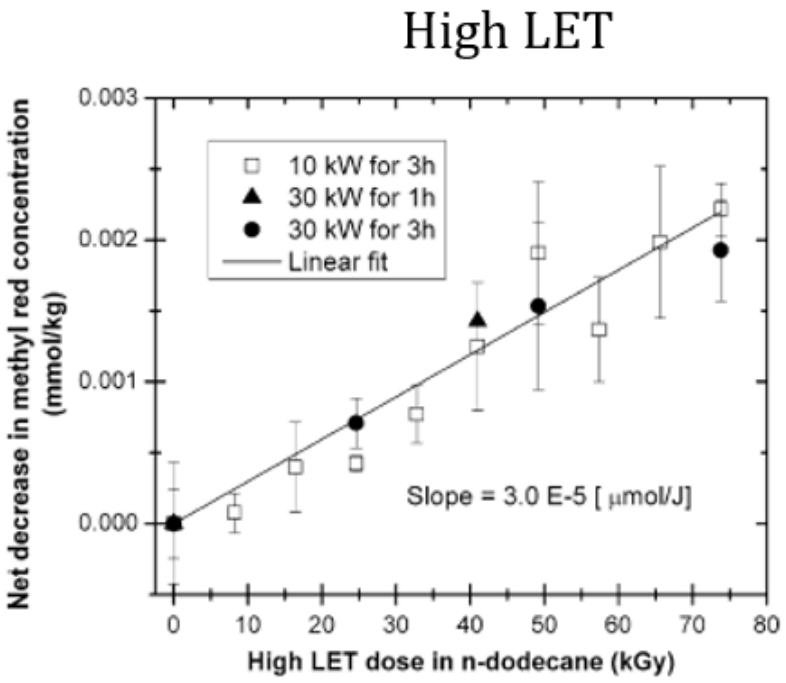

Figure 34. Various high LET (TRIGA^{TM}) α irradiation of methyl red in dodecane. Solid line is computer model fit. Degradation efficiency fitted as 3.0 x 10^{-5} μmol J^{-1} at room temperature.

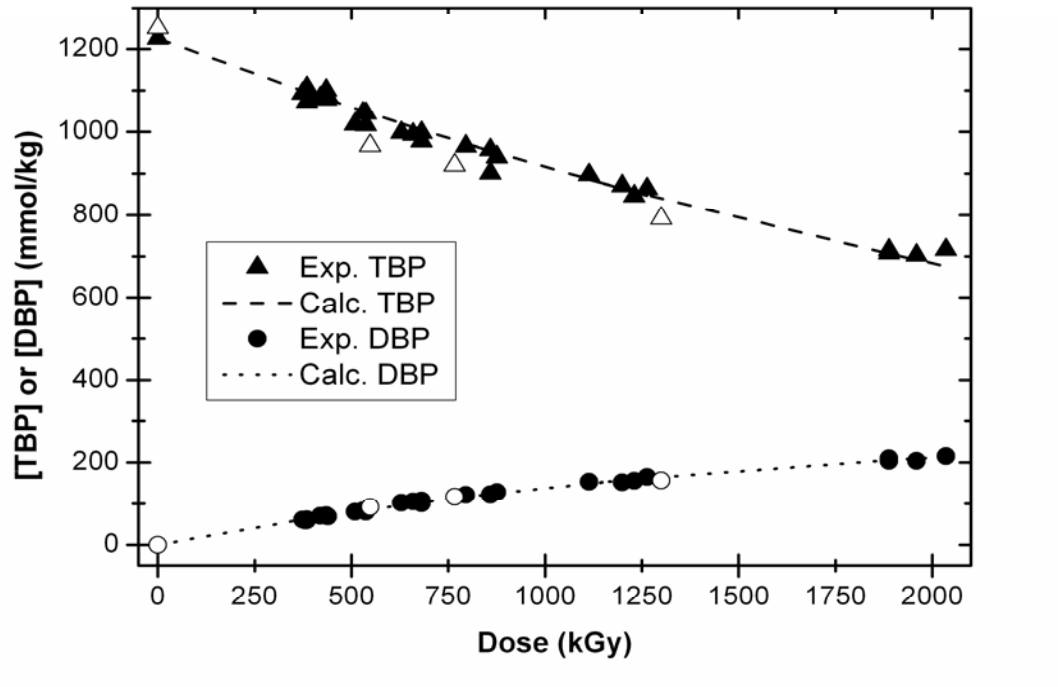

Figure 35. TRIGA™ based high LET-irradiated TBP in dodecane. Dashed and dotted lines are the results of computer modeling of this system to give the G-values listed in Table 6.

Table 6. Measured *G*-values (μmol Gy^{-1}) for high-LET irradiation of TBP in dodecane

Reaction path	γ irradiation	α irradiation
Degradation of TBP to all products	0.36	0.14
Degradation of TBP to DBP, i.e. formation of DBP	0.18	0.047

For TBP degradation, both the loss of TBP and the production of the product dibutyphosphate (DBP) could be directly monitored by gas chromatography (GC). Typical data[36] for the reactor alpha irradiation are shown in Figure 35. Based on the deconvolution computer model, individual *G*-values for both TBP loss and DBP production and subsequent loss could be determined (see Table 6). The computer model predicted loss/production is also shown in Figure 33, with excellent agreement observed. From the data in Table 6 it is also clear to see that almost half the TBP loss does not lead to DBP for γ irradiation, and even less occurs by this pathway for α irradiation.

There have been multiple previous *G*-value determinations for TBP radiolysis, mainly by low and a few for high LET particles. Representative data are shown in Tables 7 and 8, and are compared to the data of this study.

Table 7. Comparison of TRIGA™ low LET irradiation data with previous literature for TBP.

Source	Reference	Solution	Irradiation Conditions	G^{+}_{DBP} (µmol/J)
^{137}Cs	**This study**	1M TBP/n-dodecane	No pretreatment, 'dry'	**0.18**
^{60}Co	37	30% TBP/isooctane	No pretreatment, 'dry'	0.19
^{60}Co	38	30% TBP/decane	No pretreatment, 'dry'	0.15
^{90}Sr	39	30% TBP/alkane	In contact with 3M HNO_3	0.11
^{60}Co	40	30% TBP/kerosene	Pre-equilibrated 3M HNO_3	0.10
Low LET	41	30% TBP in Aliphatic Diluents	H_2O Saturated	0.09

Table 8. Comparison of TRIGA™ low LET irradiation data with previous literature for TBP.

Source	Reference	Solution	Irradiation Conditions	G^{+}_{DBP} (µmol/J)
$^{10}B(n,\alpha)^{7}Li$	**This study**	1M TBP/n-dodecane	Sealed in polyvials "Dry"	**0.063**
Helium ion	42	30% TBP/n-dodecane	Sealed in quartz "Dry"	0.07
Pu^{238}	40	30% TBP/ kerosene	Pre-equilibrated 3M HNO_3	0.08
Pu^{238}	43	30%TBP/n-dodecane	Pre-equilibrated 3M HNO_3	0.09
Pu^{238}	44	30% TBP/n-dodecane	Pre-equilibrated 3M HNO_3	0.10
Pu^{238}	45	30% TBP/paraffin	In contact with 3M HNO_3	0.10

Overall, alpha radiolysis causes less TBP degradation than gamma radiolysis. For γ irradiation excellent agreement is seen for the "dry" irradiation values. Solutions that were in contact with acid and/ or water show much lower DBP formation G-values. The G-values for DBP formation from alpha radiolysis (Table 8) are much more varied, but the only directly comparable value for "dry" irradiation is in pretty good agreement. In this situation, having pre-contact with HNO_3 appears to increase the degradation of TBP to DBP.

4.4.1 Uranium loaded TBP degradation studies

A number of subsequent experiments were carried out with solutions of TBP in n-dodecane loaded with varying concentration of uranyl nitrate. In parallel were studies using TBP/n-dodecane solutions contacted with nitric acid and some 'dry', i.e. not contacted with any aqueous phase. All solutions were prepared with or without boron compounds for subsequent high-LET studies. The TBP concentration was 0.1 M in n-dodecane. This lower TBP concentration was chosen so that we could observe high loading of uranium in the organic solution, i.e. having a relatively high U:TBP ratio. However, these conditions resulted in larger measurement uncertainties and no possible detection of DBP degradation product.

The organic solutions were contacted with 3 M nitric acid containing varying concentration of uranyl nitrate, ranging from 0 to 0.1 M. The aqueous phase was removed after contact and the organic solutions then irradiated. One set of these solutions was irradiated in a ^{137}Cs irradiator to various gamma doses, with samples taken before irradiation, and then every 7 days up to 28 days of total exposure. A blank set of solutions was also run to determine TBP degradation due to acid or metal hydrolysis. A third set of samples was placed in the TRIGA^{TM} reactor at different irradiation times to match the total high LET dose to that of the γ irradiation. Correction for the γ irradiation experienced by the samples in the reactor was performed using solutions that had no boron included.

All samples were analyzed by in-house GC by diluting the samples in hexane and adding a derivatizing agent to ensure that all degradation products would be sufficiently volatile. Figure 36 shows the TBP concentration from samples contacted with 0.05 M uranyl nitrate and irradiated in the gamma-source. Figure 37 shows similar samples irradiated in the reactor with the presence of boron. Immediately, it can be seen that the concentration of TBP is lower than 0.1 M. This is attributed to the metal loading; it is assumed that each uranyl ion is coordinated by two TBP molecules. Indeed, activation analysis to establish the uranium concentration in each organic phase verified that the free TBP concentration matches well that measured by GC if the assumption that UO_2^{2+} ions in the organic phase reduce the free TBP in a 1:2 ratio. This also leads us to believe that the GC analysis method is not able to break up the TBP_2-UO_2-NO_3 complexes, and hence we are analyzing only free TBP.

The free TBP present in the irradiated samples is calculated by first assuming that TBP degrades by gamma radiation. TBP/n-dodecane solutions contacted with only nitric acid but without uranium and exposed in the Cs-source were used to find the degradation constant for this path. The second assumption required to accurately model the observed decay concentrations was that each TBP_2-UO_2-NO_3 complex that degrades releases one TBP molecule resulting in an increase in the free TBP concentration. The degradation constant for the TBP-metal complex was obtained by fitting the free TBP data at each metal concentration. It was assumed that gamma degradation of free TBP would have the same value regardless of the metal concentration.

Once degradation constants for the low LET constants were established the equivalent constants for high LET were calculated. Finally, the TBP data for uranium loaded organic phases containing boron and irradiated in the reactor was fitted. The degradation of free TBP matched reasonably well with the values already established previously (see last section). Slight differences were observed which might be attributed to the fact that the solutions are contacted with nitric acid and that the starting concentration was much lower. It can be seen that the high LET has a smaller effect than low LET Table 9). Furthermore, the TBP-U complex degrades more quickly than free TBP. This is the reason for the apparent increase in free TBP concentration during irradiation when TBP-U complexes are present.

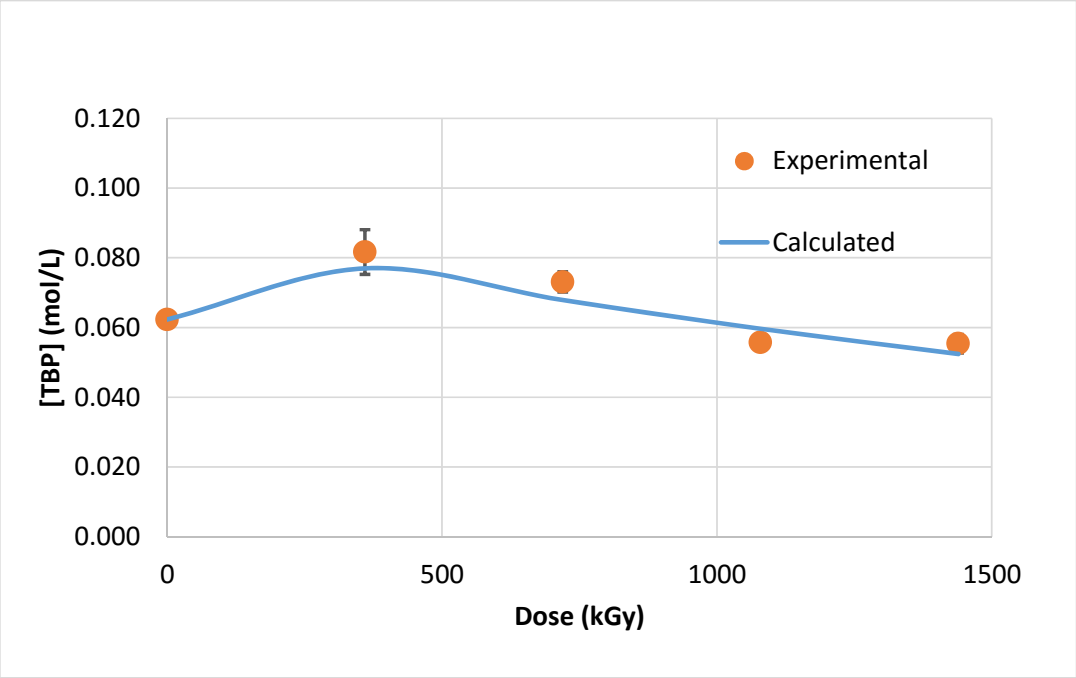

Figure 36. Free TBP concentration for samples contacted with 0.05 M uranyl nitrate in 3 M HNO_3. Total TBP before contact was 0.1 M and the solvent was n-dodecane. Cs-137 gamma irradiation only.

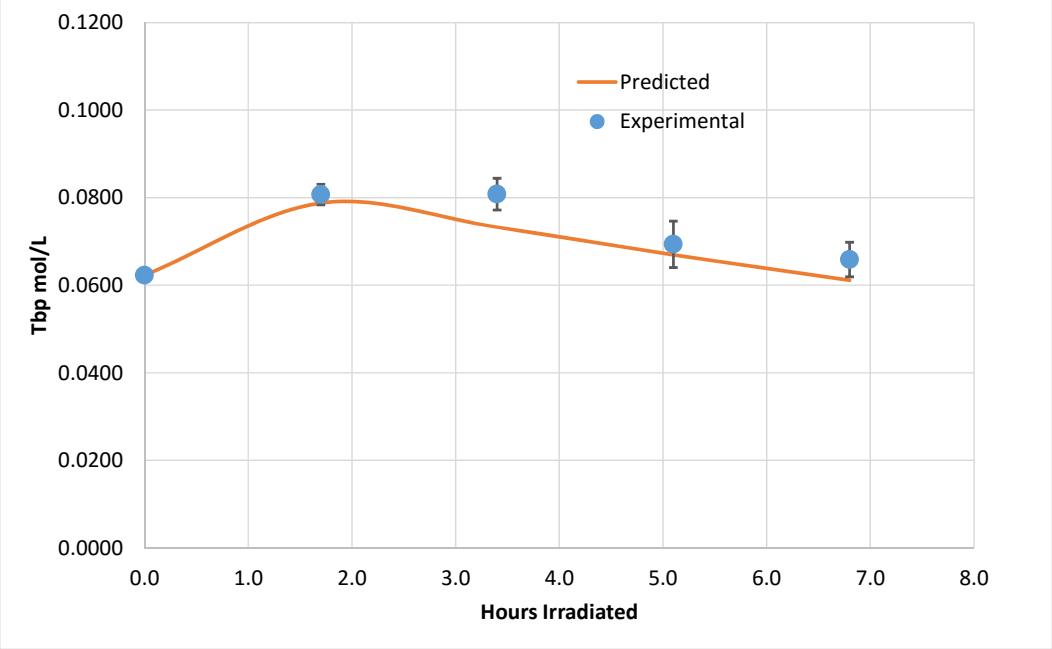

Figure 37. Free TBP concentration for samples contacted with 0.05 M uranyl nitrate in 3 M HNO_3. Total TBP before contact was 0.1 M and the solvent was n-dodecane, bis-pinacolato diboron was included in all the samples to match the low LET doses shown in Figure 36.

Table 9. Degradation constants for free TBP and TBP-U complex using high and low LET irradiation.

Irradiation Condition	Value (kGy^{-1})
Degradation of the TBP-U complex by gamma	1.26×10^{-2}
Degradation of free TBP by gamma	3.59×10^{-4}
Degradation of the TBP-U complex by high LET	3.8×10^{-3}
Degradation of free TBP by high LET	1.86×10^{-4}

4.5 Methylene blue irradiation studies

One of the most important milestones of this proposal was to identify the best alpha-radiolysis technique. While it is recognized that "the best" is a broad category, it was important that each alpha radiolysis methodology gave the same result, and that ease of use and availability of the method were also considered. The data detailed previously for CMPO, DTPA and TBP all showed excellent stability in organic media, particularly acidic aqueous-contacted organic media. This meant that only the ^{244}Cm and reactor irradiations could be used to perform these experiments, as the ion-beam and ^{211}At irradiations did not provide sufficient total dose to degrade these compounds in a measurable quantity. This is another reflection of the less deleterious effects of high LET radiation on solvent extraction ligands.

Therefore, to fully examine the capabilities of each alpha irradiation approach, a more sensitive system requiring less dose for compound degradation was incorporated. The system chosen for study was methylene blue, see Figure 38, a water soluble dye that had already been shown to undergo radiolytic-degradation at doses less than 1 kGy. In addition, one high LET irradiation study had already been performed on this dye, with the obtained data shown in Figure 39[46]. The same batch of chemical was used for all experiments.

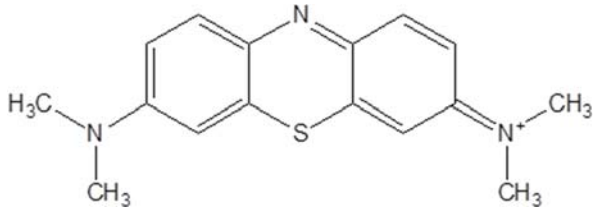

Figure 38. Chemical structure of the dye methylene blue used for high LET irradiation comparison.

For this study, all four types of high LET irradiation were conducted on this dye molecule in water. Unfortunately, while the ^{211}At experiments were performed, no meaningful degradation data could be elucidated from the UV-visible spectra taken 3-5 days after the irradiation occurred. A new, strong, absorbance in the far visible was observed, which we attributed to the daughter Bi forming a complex with the methylene blue dye, or some of its degradation products. Deconvolution of the overall absorbance to obtain just the remaining methylene blue absorbance has not yet been successful. Attempts to further analyze these data are on-going.

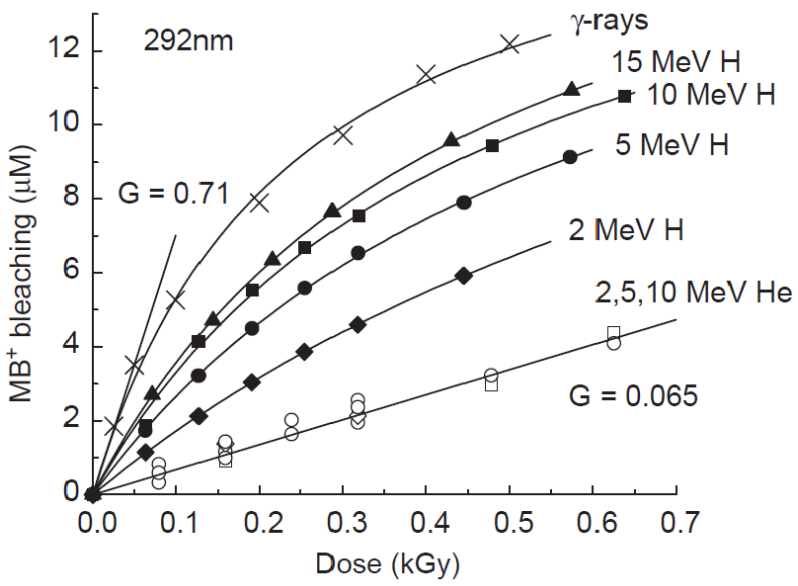

Figure 39. Literature[46] data for the high LET radiolysis of 16 μM methylene blue in neutral aqueous solution. Of particular relevance are the two limiting values, listed as G = 0.71 value for γ-rays, and the G = 0.065 #molecules/100eV for 2, 5 and 10 MeV He^{2+} ions. Note that these G-value units are pre-SI, to convert these units to μmol J^{-1} multiply by 0.1013. For example, 0.065 #molecules/100eV = 0.0071 μmol J^{-1}.

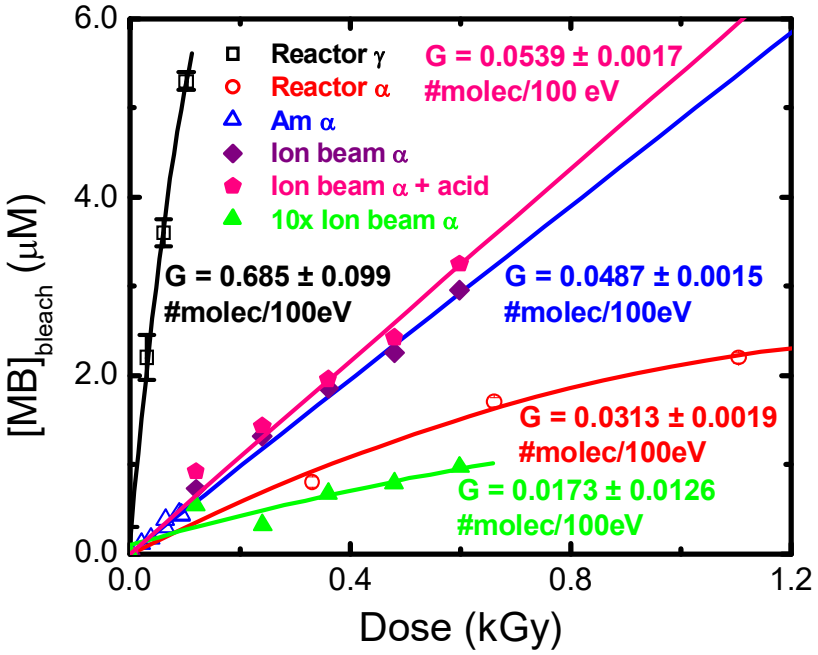

Figure 40. Summary of alpha irradiations performed for methylene blue dye (16 μM, pH 0 - 7) in this study. G-values in units of #molecules/100eV to be consistent with previous literature data[46].

Table 10. Summary of *G*-values obtained for methylene blue high LET irradiation.

Method	G-value (μmol Gy^{-1})
2,5,10 MeV He ion beam (2005)	0.00710 ± 0.00050
5 MeV He ion beam (2014)	0.00539 ± 0.00017
5 MeV He ion beam + 0.10 M acid (2014)	0.00491 ± 0.00082
^{243}Am isotope (2015)	0.00487 ± 0.00015
Reactor α (2014)	0.00313 ± 0.00019

The remaining high LET irradiations, ^{243}Am, 5 MeV He ion beam and the TRIGA^{TM} reactor all gave meaningful data, these are shown in Figure 40. Excellent agreement was seen between the Am isotope alpha irradiation and the helium ion beam, at low dose, for both neutral pH and 0.10 M HNO_3 conditions. The *G*-values obtained, 0.049 – 0.054 #molecules/100 eV can be considered equal within experimental error. The new alpha degradation value by these methods is slightly lower than previously measured, however, this can be attributed to different batch used for this dye. The TRIGA^{TM} gamma de-convoluted value is also shown in Figure 38, the calculated gamma *G*-value of 0.69 #molecules/100 eV is in very good agreement with the published value of G = 0.71 #molecules/100eV shown in Figure 39. However, the TRIGA^{TM} high LET data were far lower; taking the initial slope of these curved data gives G = 0.031 #molecules/100 eV? Insight into this significant difference was obtained by repeating the He ion beam irradiation at a dose rate that was 10x higher than the original irradiation. Under the high dose rate conditions, a much lower (and curved, like the TRIGA^{TM} data) G-value of 0.017 #molecules/100 eV was obtained. All these conditions are summarized in Table 10 (also converted to SI units). We attribute the lower value for the high LET irradiation of the TRIGA^{TM} reactor to the relatively high dose rate of irradiation. It would be desirable to perform additional experiments at different dose rates to allow a quantitative extrapolation to zero-dose, to see if better agreement with the ion-beam/Am isotope data can be achieved.

5. CONCLUSION

The work performed here measured and compared the impacts of γ and α- irradiation on ligands used in separation systems for nuclear applications. Effort was focused upon the major ligands used in the PUREX, TRUEX and TALSPEAK processes, notably TBP, CMPO and DTPA. The major goal of this proposal was to quantitatively compare low linear energy transfer (low LET, γ-irradiation) and high linear energy transfer (high LET, α-irradiation) on diluents (dodecane) and ligands, both free and metal-loaded. These comparisons were achieved in this work.

Under fully-aerated, acidic, conditions in the aqueous phase, the most important radicals were the hydroxyl radical ($HO^{\bullet}$) and the nitrate radical ($^{\bullet}NO_3$). Hydroxyl radical rate constants were determined for DTPA, and metal loaded-DTPA using electron pulse radiolysis/transient absorption techniques and SCN^-

competition kinetics. From the rate constant data measured in this work over a range of pH and temperature individual DTPA species rate constants and Arrhenius/Eyring parameters were obtained for the free ligand. For pH < 4 all DTPA protonated species reacted equivalently, only at pH 6.0, where the H_2DTPA^{2-} species dominated were different kinetics and thermodynamics found. The lanthanide-loaded DTPA species all reacted much more quickly than the free DTPA, but in this case it was the most acidic pH's that showed different behavior. For $^{\bullet}NO_3$ radical reactivity in the aqueous phase, reaction rate constants were directly measured following the radical absorbance at 630 nm. Rate constants varied over many orders of magnitude, being fastest when aromatic rings with methyl substituents were present. The $^{\bullet}NO_3$ radical absorbance in organic media (*tert*-butanol, as no $^{\bullet}NO_3$ radical source could be found for dodecane) was very similar to that of the aqueous phase, and so the same method of measurement was employed. Overall, it was seen that $^{\bullet}NO_3$ reactions with ligands in the organic phase occurred more quickly than in the aqueous phase. Like the hydroxyl radical with metal-loaded DTPA $^{\bullet}NO_3$ reactions with metal-loaded ligands (CMPO) in the organic phase were even faster. Lastly in the organic phase kinetics of the dodecane solvent radical cation ($C_{12}H_{26}^{+\bullet}$) were measured for CMPO, showing almost diffusion-controlled reaction rates.

These kinetic data were augmented by steady-state irradiations on diluents and solvent systems, where distribution and stripping ratios and mass spectrometric measurements of decomposition products were determined. While gamma irradiation was performed using either ^{60}Co or ^{137}Cs irradiators three distinctly different methods for alpha radiolysis were utilized. These included isotopic alpha irradiation (^{244}Cm, ^{243}Am, ^{211}At), helium ion beam irradiation (5.0 MeV He^{2+} accelerated particles) and a TRIGA™ reactor. Primary focus was on CMPO in dodecane, particularly solutions that had been pre-contacted with nitric acid aqueous systems, where a remarkable increase in radiation stability was found. This was attributed to the formation of a $[CMPO_x \bullet (HNO_3)_{y+1}]$ complex, $K_{eq} = 0.15 \pm 0.01$, that gave additional protection to this ligand from radical degradation. Mass spectroscopy analysis of irradiated CMPO/dodecane systems showed different breakdown patterns and product distribution yields for the two forms of radiation, indicating that different reaction mechanisms were occurring for low and high LET irradiation. No difference for dodecane radical cation reactivity with dry CMPO or pre-contacted CMPO was found. These product studies were augmented by a detailed study of forward extraction distribution coefficient value, and stripping value, measurements for both forms of irradiation.

The kinetic findings above for metal-loaded ligands were also observed in reactor based uranium-TBP radiolysis experiments. It was seen that gamma irradiation caused generally much more degradation than alpha irradiation, and that uranium complexed TBP degraded far quicker than the free TBP ligand itself. Quantitative compute modeling of these experimental degradation systems was also performed, with specific *G*-values elucidated.

The excellent radiation stability of these ligands, while an excellent finding for future large-scale reprocessing work, meant that direct comparison of the different alpha-radiolysis techniques for them was not possible. Ultimately, a direct comparison of these three alpha irradiation techniques on a model dye, methylene blue, demonstrated that dose-rate effects were extremely important in quantifying the overall degradation efficiencies. Excellent agreement was obtained for isotope (^{243}Am) plus ion-beam alpha irradiation, but the higher dose rates for the TRIGA™ reactor gave considerably lower values. Based on these dye data we suggest that the most advantageous method to be used for future alpha radiolysis would be the He ion beam irradiation.

One other planned product of this work was to collate the experimental information for these ligands into a computer model. However, the excellent radiation stability of TBP and CMPO for alpha radiolysis, particularly for the latter when pre-contacted with acid, suggests that the predicted use of these chemicals only requires an empirical loss calculation which would be based on specific operating conditions. This should considerably simplify future modeling efforts in this area.

The knowledge gained in this work provides not only a comprehensive understanding of the radiation chemistry of currently proposed processes, but also give quantitative baseline information and evaluation methods for any future proposed nuclear solvent extraction systems. Thus this study filled major current gaps that had existed for real-world, irradiated, solvent systems.

6. REFERENCES

1. *Actinide and fission product partitioning and transmutation-states and assessment report,* (**OECD-NEA**), Paris, (1999).
2. Weaver, B.; Kappelmann, F.A., *TALSPEAK, A new method of separating americium and curium from the lanthanides by extraction from an aqueous solution of an aminopolyacetic acid complex with a monoacidic organophosphate or phosphonate*, **ORNL-3359**, (1964).
3. Mincher, B.J.; Modolo, G.; Mezyk, S.P., *The Effects of Radiation Chemistry on Solvent Extractions: 3. A Review of Actinide and Lanthanide Extraction* **Solv. Ext. Ion Exch.**, *27*, 579-606, (2009).
4. Sasaki,Y.; Sugo, Y.; Suzuki, S.; Kimura, T., *A method for the determination of extraction capacity and its application to N,N,N',N'-tetraalkylderivatives of diglycolamide-monoamide/n-dodecane media*, **Anal. Chim. Acta**, *543*, 31-37, (2005).
5. Gelis, A.V.; Lumetta, G.J., *Actinide Separation Process – ALSEP.* **Indus. Engineer. Chem. Res**., *53*, 1624-1631, (2014).
6. Pikaev, A.K.; Kabakchi, S.A.; Egorov, G.F., Some radiation chemical aspects of nuclear engineering. **Radiat. Phys. C**hem., *31*, 789-803, (1988).
7. https://www.orau.org/PTP/PTP%20Library/library/DOE/bnl/nuclidedata/MIRAt211.htm, accessed August 01, 2015.
8. LaVerne, J.A., Schuler, R.H., *Radiation chemical studies with heavy ions: oxidation of ferrous ion in the Fricke dosimeter*. **J. Phys. Chem**. 91, 5770-5776, (1987).
9. Pearson, J., Jan, O., Miller, G. E., Nilsson, M., *Studies of high linear energy transfer dosimetry by $^{10}B(n,\alpha)^{7}Li$ reactions in aqueous and organic solvents*. **J. Radioanal. Nucl. Chem.,** *292(2)*, 719-727, (2012).
10. Toney, W.M.; Waltner, A.W., *An investigation of the $^{10}B(n,\alpha)^{7}Li^{*}$, ^{7}Li reaction branching ratio.* **Nucl. Phys**. *80*, 237-240 (1966).
11. Elias, G.; Groenewold, G.S.; Mincher, B.J.; Mezyk, S.P., *Determination of CMPO and Identification of some Radiolysis Products using HPLC-UV and Mass Spectrometry*. **J. Chromatog. A**, *1243*, 47-52, (2012).
12. Nash, K.L.; Gatrone, R.C.; Clark, G.A.; Rickert, P.G.; Horwitz, E.P., *Hydrolytic and radiolytic degradation of CMPO: Continuing studies*. **Sep. Sci. Technol**. *23*, 1355-1372, (1988).
13. Mincher, B.J.; Mezyk, S.P.; Groenewold, G.S.; Elias, G., *A comparison of the alpha and gamma radiolysis of CMPO*, **INL/EXT-11-22632**, June (2011).

14. Fuji, T.; Aoki, K.; Yamana, H., *Effect of nitric acid distribution on extraction behavior of trivalent f-elements in a TRUEX system*. **Solvent Extr. Ion Exch**. *24* 347-357, (2006).
15. Horwitz, E.P.; Diamond, H.; Martin, K.A.; Chiarizia, R., *Extraction of americium (III) from chloride media by octyl(phenyl)-N,N-diisobutylcarbamoylmethylphosphine oxide.* **Solv. Extr. Ion Exch**. *5* 419-446, (1987).
16. Chaiko, D.J.; Fredrickson, D.R.; Reichley-Yinger, L.; Vandegrift, G.F., *Thermodynamic modeling of chemical equilibria in metal extraction*. **Sep. Sci. Technol**. *23*, 1435-1451, (1988).
17. Buxton, G.V.; Greenstock, C.L.; Helman, W.P.; Ross, A.B., *Critical review of rate constants for reactions of hydrated electrons, hydrogen atoms and hydroxyl radicals (·OH/·O⁻) in aqueous solution***. J. Phys. Chem. Ref. Data**, *17*, 513-886, (1988).
18. Katsumura, Y.; Jiang, P.Y.; Nagaishi, R.; Oishi, T.; Ishigure, K.; Yoshida, Y., Pulse radiolysis study of aqueous nitric acid solutions. Formation mechanism, yield, and reactivity of NO_3 radical **J. Phys. Chem**., *95*, 4435-4439, (1991).
19. Lefort M.; Tarrago X., *Radiolysis of water by particles of high linear energy transfer. The primary chemical yields in aqueous acid solutions of ferrous sulfate, and in mixtures of thallous and ceric ions*. **J. Phys. Chem**. *63*, 833-836, (1959).
20. Mincher, B.J.; Mezyk, S.P.; Elias, G.; Groenewold, G.S.; Riddle, C.L.; Olson, L.G., *The radiation chemistry of CMPO: Part 1. Gamma radiolysis*, **Solv. Ext. Ion Exch.**, 7, 715-730, (2013).
21. Simonzadeh, N.; Crabtree, A.M.; Trevorrow, L.E.; Vandegrift, G.F., *Radiolysis and hydrolysis of TRUEX-NPH solvent*. Argonne National Laboratory Report **ANL-90/14**, July (1992).
22. Logunov, M.V.; Voroshilov, Yu. A.; Starovoitov, N.P.; Shadrin, A.Yu.; Smirnov, I.V.; Kvasnitskii, I.B.; Tananaev, I.G. ; Myasoedov, B.F.; Morgalyuk, V.P.; Kamiya, M.; Koma, I.; Koyama, T. *Radiation resistance of a series of organophosphorous extractants*. **Radiochemistry** *48*, 55–61, (2006).
23. Chiarizia, R.; Horwitz, E.P., *Hydrolytic and radiolytic degradation of octyl(phenyl)-N,Ndiisiobutylcarbamoylmethylphosphine oxide and related compounds*. **Solv. Ext. Ion Exch**. *4*, 677–723, (1986).
24. Nash, K.L.; Rickert P.G.; Horwitz, E.P. *Degradation of TRUEX-dodecane process solvent*. **Solvent Extr. Ion Exch**. *7*, 655–675, (1989).
25. Mincher, B.J.; Mezyk, S.P.; Elias, G.; Groenewold, G.S.; LaVerne, J.A.; Nilsson, M.; Pearson, J.; Schmitt, N.C., *The Radiation Chemistry of CMPO: Part 2. Alpha Radiolysis.* **Solv. Ext. Ion Exch.**, 32, 167-178, (2014).
26. Pearson, J.; Jan, O.; Wariner, A.; Miller, G.E.; Nilsson, M., *Development of a method for high LET irradiation of liquid systems*. **J. Radioanal. Nucl. Chem.** *258*, 1401–1409, (2013).
27. Ziegler, J.F.; Biersbak, J.P.; Littman, U. *The Stopping and Range of Ions in Solids*; 1985, Pergamon Press: New York, NY.
28. Spinks J.W.T.; Woods, R.J. *An Introduction to Radiation Chemistry*, 3rd ed.; 1991; John Wiley and Sons: Hobokken, NJ.
29. Camès, B.; Bisel, I.; Baron, P.; Hill, C.; Rudloff, D.; Saucerotte, B. DIAMEX solvent behavior under continuous degradation and regeneration operations. In *Nuclear Energy and the Environment*; Wai, C.M., Mincher, B.J., Eds.; ACS Symposium Series 1046, American Chemical Society, Washington, D.C., pp 255–270 (2010).
30. Groenewold, G. S.; Elias, G.; Mincher, B.J.; Mezyk S.P.; LaVerne, J.A., *Characterization of CMPO and its radiolysis products by direct infusion ESI-MS*. **Talanta** *99*, 909–917, (2012).

31. Wishart, J.F.; Cook, A.R.; Miller, J.R. *The LEAF picosecond pulse radiolysis facility at Brookhaven National Laboratory*. **Rev. Sci. Instrum**. 75, 4359-4436, (2004).
32. Zarzana, C.A.; Groenewold, G.S.; Mincher, B.J.; Mezyk, S.P.; Wilden, A.; Schmidt, H .; Modolo, G.; Wishart, J.F.; Cook, A.R., *A Comparison of the γ-radiolysis of TODGA and T(EH)DGA using UHPLC-ESI-MS Analysis.* **Solv. Extr. Ion Exch**., *33*, 431-447, (2015).
33. Mezyk, S.P.; Mincher, B.J., Dihman, S.B.; Layne, B.; Wishart, J.F., *The role of organic solvent radical cation in separations ligand degradation.* **J. Radioanal. Nucl. Chem.,** *307*, 2445-2449, (2016).
34. NIST Standard Reference Database 46: NIST Critically selected stability constants of metal complexes. Version 8.0, 2004.
35. Pearson, J.; Jan, O.; Wariner, A.; Miller, G. E.; Nilsson, M., *Development of a method for high LET irradiation of liquid systems*. **J. Radioanal. Nucl. Chem**., *298(2)*, 1401-1409, (2013).
36. Pearson, J.; Nilsson, M., *Radiolysis of tributyl phosphate by particles of high linear energy transfer*. **Solv. Ext. Ion Exch.**, *32(6)*, 584-600, (2014).
37. Burger, L. L., *Uranium and plutonium extraction by organophosphorus compounds*. **J. Phys. Chem**., *62*, 590-593, (1958).
38. Egorov, G. F.; Tkhorzhnitskii, G. P.; Zilberman, B. Ya.; Shmidt, O. V.; Goletskii, N. D., *Radiation chemical behavior of tributyl phosphate, dibutylphosphoric acid, and its zirconium salt in organic solutions and two-phase systems*. **Radiochemistry** (New York, NY, United States) *47*, 392-397, (2005).
39. Becker, R.; Stieglitz, L.; Bautz, H., *Radiolytic TBP degradation under PUREX process conditions.* **Kernforschungszent** Karlsruhe, 50 pp. (1983)
40. Li, H. –B.; Su, Z.; Cong, H. –F.; Lin, C. –S., *α and γ irradiation stability of 30%TBP-Kerosene-HNO_3 systems*. **J. Radioanal. Nucl. Chem.** *34*, 281-285, (2012).
41. Schulz, W.W.; Navratil, J.D., *Science and technology of tributyl phosphate. Vol. I: Synthesis, properties, reactions and analysis*. **CRC Press**, Boca Raton, FL (1984).
42. Ladrielle, T.; Wanet, P.; Lemaire, D.; Apers, D. J., *Alpha and gamma induced radiolysis of tributyl phosphate*. **Radiochem. Radioanal. Lett**., *59*, 355-63 (1983).
43. Kawaguchi, Y.; Morimoto, K.; Kitao, T.; Ohyama, K.; Omori, E., *Study of solvent degradation in reprocessing MOX spent fuel: solvent degradation and its effect on Pu purification cycle.* **Nihon Genshiryoku Gakkai Wabun Ronbunshu** *8*, 221-229 (2009).
44. Lloyd, M. H.; Fellows, R. L., Alpha radiolysis and other factors affecting hydrolysis of tributyl phosphate. Report ORNL/TM-9565; Order No. DE85015071), 25 pp, (1985).
45. Kulikov, I. A.; Kermanova, N. V.; Vladimirova, M. V., *Radiolysis of tributyl phosphate in the presence of plutonium and uranium*. **Radiokhimiya**, *25*, 330-336, (1983).
46. LaVerne, J.A.; Tandon, L.; Knippel, B.C.; Montoya, V.M., **Radiation Physics and Chemistry**, 72, 143-147, (2005).

7. INDICATORS OF PROJECT QUALITY

1) *Publications generated from the work of this proposal:*

Peer-reviewed journal publications:

1. Mezyk, S.P.; Mincher, B.J.; Dihman, S.B.; Layne, B.; Wishart, J.F., *The role of organic solvent radical cations in separations ligand degradation.*, **J. Radioanal. Nucl. Chem.,** 307, 2445-2449, (2016).
2. Wilden, A.; Modolo, G.; Hupert, M.; Santiago-Schubel, B.; Lofstrom-Engdahl, E.; Hallerod, J.; Ekberg, C.; Mincher, B.J.; Mezyk, S.P., *Gamma-radiolytic stability of solvents containing C5-BPP (2,6-Bis(5-(2,2-dimethylpropyl)-1H-pyrazol-3-yl) pyridine) for actinide(III)/lanthanide(III) separation.* **Solv. Ext. Ion Exch.** 34, 1-12, (2016).
3. Pearson, J.; Nilsson, M., *Radiolysis of tributyl phosphate by particles of high linear energy transfer*. **Solv. Ext. Ion Exch.***, 32(6)*, 584-600, (2014).
4. Zarzana, C.A.; Groenewold, G.S.; Mincher, B.J.; Mezyk, S.P.; Wilden, A.; Schmidt, H .; Modolo, G.; Wishart, J.F.; Cook, A.R., *A Comparison of the γ-radiolysis of TODGA and T(EH)DGA using UHPLC-ESI-MS Analysis.* **Solv. Extr. Ion Exch**., *33*, 431-447, (2015).
5. Mincher, B. J., Mezyk, S. P., Elias, G., Groenewold, G. S., LaVerne, J. A., Nilsson, M**.**, Pearson, J., Schmitt, N. C., Tillotson, R. D., Olson, L. G., T*he radiation chemistry of CMPO: Part 2. Alpha radiolysis.* **Solv. Ext. Ion Exch.***, 32(2)*, 167-178, (2014).
6. Mincher, B.J.; Mezyk, S.P.; Elias, G.; Groenewold, G.S.; Riddle, C.L.; Olson, L.G., *The Radiation Chemistry of CMPO: Part 1. Gamma Radiolysis*, **Solv. Ext. Ion Exch**., *7*, 715-730, (2013).
7. Pearson, J.; Jan, O.; Wariner, A.; Miller, G. E.; Nilsson, M., *Development of a method for high LET irradiation of liquid systems*. **J. Radioanal. Nucl. Chem***., 298(2)*, 1401-1409, (2013).
8. Mezyk, S.P.; Mincher, B.J.; Ekberg, C.; Skarnemark, G., *Alpha and gamma radiolysis of nuclear solvent extraction ligands used for An(III) and Ln(III) separations*, **J. Radioanal. Nucl. Chem**., *296*, 711-715, (2013).
9. Cullen, T.D.; Mezyk, S.P.; Martin, L.R.; Mincher, B.J., *Elucidating the Radical Kinetics Involved in the Radiolytic Destruction of Lanthanide-Complexed DTPA Separations*, **J. Radioanal. Nucl. Chem.**, *296*, 717-720, (2013).
10. Groenewold, G.S.; Elias, G.; Mincher, B.J.; Mezyk, S.P.; LaVerne, J.A., *Characterization of CMPO and its radiolysis products by direct infusion ESI-MS*, **Talanta**, *99*, 909-917, (2012).
11. Elias, G.; Groenewold, G.S.; Mincher, B.J.; Mezyk, S.P., *Determination of CMPO and identification of some radiolysis products using HPLC-UV and Mass Spectrometry*. **J. Chromatog. A**, *1243*, 47-52, (2012).
12. Jan, O.; Miller, G. E.; Nilsson, M., *Studies of high linear energy transfer dosimetry by $^{10}B(n,\alpha)^{7}Li$ reactions in aqueous and organic solvents*. **J. Radioanal. Nucl. Chem.**, *292(2)*, 719-727, (2012).
13. Swancutt, K.L.; Cullen, T.D.; Mezyk, S.P.; Elias, G.; Bauer, W.F.; Peterman, D.R.; Riddle, C.L.; Ball, R.D.; Mincher, B.J.; Muller, J.J., *The radiation chemistry of the Cs-7SB modifier used in Cs and Sr solvent extraction,* **Solv. Ext. Ion Exch**. *29*, 106-127 (2011).
14. Elias, G.; Mincher, B.J.; Mezyk, S.P.; Muller, J.; Martin, L.R., *Toluene Nitration in Irradiated Nitric Acid and Nitrite Solutions*, **Rad. Phys. Chem**. *80*, 554-560 (2011).

Peer-reviewed conference publications:

1. Nilsson, M.; Pearson, J., *High LET radiolytic degradation of solvent extraction processes for used nuclear fuel*. In, Proceedings from the International Solvent Extraction Conference (pp. 563-568). **ISEC 2014**. Würzburg, Germany (2014).
2. Mezyk, S. P.; Mincher, B. J.; Nilsson, M.; Pearson, J.; Laverne, J. A., *The radiation chemistry of CMPO*. In, Proceedings from the International Solvent Extraction Conference. **ISEC 2014**, Würzburg, Germany, 545-550, (2014).
3. Pearson, J.; Miller, G. E.; Nilsson, M., *Alternative methods for degradation studies by alpha radiolysis: Tributyl phosphate and CMPO*. In, Nuclear Energy at a Crossroads. **GLOBAL-2013**: International Nuclear Fuel Cycle Conference. Salt Lake City, USA (2013).
4. Pearson, J.; Miller, G. E., *High linear energy transfer degradation studies simulating alpha radiolysis of TRU solvent extraction processes*. ASME 2103 15th International Conference on Environmental Remediation and Radioactive Waste Management, **ICHEM**. Brussels, Belgium (2013).
5. Pearson, J.; Jan, O.; Wariner, A.; Miller, G.; Nilsson, M., *An in-situ alpha radiolytic study of tributyl phosphate*. In, **Transactions of the American Nuclear Society,** 107, 275-276, (2012).
6. Pearson, J.; Jan, O.; Miller, G. E.; Nilsson, M., *A comparison of low and high LET (linear energy transfer) induced radiolysis of solvent extraction processes*. In, **Procedia Chemistry,** 7, 334-340 (2012).
7. Pearson, J.; Jan, O.; Luc, W.; Miller, G. E.; Nilsson, M., *Alternative methods for degradation studies by alpha radiolysis*. In, Toward and Over the Fukushima Daiichi Accident. **GLOBAL-2011**. Makuhari, Japan, (2011).
8. Pearson, J.; Jan, O.; Shaka, A. J.; Miller, G. E.; Dennison, P.; Nilsson, M., *Development of a method for in situ alpha radiolysis.* In, **Transactions of the American Nuclear Society** 104, 37-38, (2011).
9. Martin, L.R.; Mincher, B.J.; Mezyk, S.P.; Elias, G.; Tillotson, R.D., *Effects of Aqueous Phase Radiolysis on Lactic Acid under TALSPEAK Conditions*, **ACS Symposium Series 1046**: Nuclear Energy and the Environment, Vol. 1046, Chapter 20, 243-253, (2010).

2) *Conference presentations generated from the work of this proposal:*

1. Ngelale, R.; Nilsson, M., *Radiolytic degradation of extraction ligands in the presence of metal ions*, 40th Annual Actinide Separations Meeting, Del Mar, CA, USA, May 24, 2016.
2. Mezyk, S.P., *Separation ligand degradation by organic radical cations*. 40th Annual Actinide Separations Meeting, Del Mar, CA, May 24-26, 2016.
3. Nilsson, M., *High LET radiolysis using small-scale research reactors*, Radical Behavior Workshop, Idaho National Laboratory, Idaho Falls, ID, USA., July 21, 2015.
4. Mezyk, S.P., *The alpha radiolysis of CMPO: Techniques Comparisons* Radical Behavior Workshop, Idaho National Laboratory, Idaho Falls, ID, July 20-22, 2015.
5. Mezyk, S.P., *How to perform a nanosecond electron pulse radiolysis experiment to study nitrate radical kinetics.*, Radical Behavior Workshop, Idaho National Laboratory, Idaho Falls, ID, July 20-22, 2015.
6. Mezyk, S.P. *Dodecane radical cation chemistry involved in separations ligand degradation*. 2015 Northwest Regional Meeting of the American Chemical Society, Pocatello, ID, June 21-24, 2015.

7. Pearson, J.; Nilsson, M., *High LET radiolytic degradation of solvent extraction processes for used nuclear fuel*, 20th International Solvent Extraction Conference, ISEC' 2014, Würzburg, Germany, September 11, 2014.
8. Mezyk, S.P.; Mincher, B.J.; Nilsson, M.; Pearson, J.; LaVerne, J.A., *The Radiation Chemistry of CMPO*, 20th International Solvent Extraction Conference, ISEC' 2014, Würzburg, Germany., September 11, 2014.
9. Pearson, J.; Miller, G.; Nilsson, M., *Radiolytic degradation of solvent extraction processes for used nuclear fuel recycling*, 38th Annual Actinide Separations Meeting, Albuquerque, NM, USA, May 22, 2014.
10. Mezyk, S.P., *Radiation Chemistry*, FCT Material Recovery and Waste Form Development Campaign, Working Group Meeting, Oak Ridge National Laboratory, USA, April 29-30, 2014
11. Mezyk, S.P., *Alpha Radiolysis of Nuclear Solvent Extraction Ligands*, FCT Material Recovery and Waste Form Development Campaign, Working Group Meeting, Oak Ridge National Laboratory, USA April 29-30, 2014.
12. Martin, L.R.; Mezyk, S.P.; Mincher, B.J., *Degradation in minor actinide separations: Addressing the challenges of radiation chemistry*. 247th American Chemical Society National Meeting and Exposition, Dallas, TX, Mar 16-20, 2014
13. Mincher, B.J.; Mezyk, S.P., *The Radiation Chemistry of Fuel Cycle Solvent Extraction Ligands; Free Radical Reactions in Mixed Phase Systems*, AOT-19, San Diego, CA, Nov. 17-21, 2013.
14. Pearson, J.; Miller, G.; Nilsson, M., *Alternative methods for degradation studies by alpha radiolysis: Tributyl phosphate and CMPO*, Global 2013: International Nuclear Fuel Cycle Conference, Salt Lake City, UT, USA. Sep. 29 – Oct.3, 2013.
15. Martin, L.; Grimes, T.; Tillotson, R.; Mezyk, S.P.; *Radiation induced degradation kinetics of next generation actinide/lanthanide separations buffers*. Global 2013, International Nuclear Fuel Cycle Conference, Salt Lake City, Sep 29 – Oct -3, 2013.
16. Pearson, J.; Jan, O.; Wariner, A.; Miller, G.; Nilsson, M., *High LET radiolytic degradation studies of separation processes for spent nuclear fuel*, 5th Asia-Pacific Symposium on Radiochemistry, APSORC'13, " Kanazawa, Japan, Sep. 22 – 27, 2013.
17. Pearson, J.; Miller, G.E.; Nilsson, M., *High linear energy transfer degradation studies simulating alpha radiolysis of TRU solvent extraction processes*, ASME 2013, 15th International Conference on Environmental Remediation and Waste Management, Brussels, Belgium, Sep. 08 – 12, 2013.
18. Pearson, J.; Miller, G.; Nilsson, M., *Degradation of TBP and CMPO in the presence of high linear energy transfer (LET) radiation*, 37th Annual Actinide Separations Meeting, Spokane, WA, USA, June 24-27, 2013.
19. Clark, A.; Pearson, J.; Nilsson, M., *Radiolysis studies of 2,2':6',2''-terpyridine*, 37th Annual Actinide Separations Meeting, Spokane, WA, USA, June 24-27, 2013.
20. Mezyk, S.P., Mincher, B.J.; Elias, G.; Precek, M.; Paulenova, A., *The Redox Chemistry of Neptunium in gamma-irradiated aqueous nitric acid*, Actinides Separation Conference, 37th Actinide Separations Conference, Spokane, WA July 2013.
21. Cullen, T.D.; Mezyk, S.P.; Martin, L.R.; Mincher, B.J., *Hydroxyl radical kinetics for metal-DTPA complexes: Size and metal charge dependence.* 245th American Chemical Society National Meeting and Exposition, New Orleans, LA, Apr 07-11, 2013.

22. Pearson, J; Jan, O.; Wariner, A.; Miller, G. E.; Nilsson, M.; *An in-situ alpha radiolytic study of tributyl phosphate*, American Nuclear Society Winter Meeting, 2012, San Diego, CA, USA, Nov 11 – 15, 2012.
23. Pearson, J.; Jan, O.; Wariner, A.; Miller, G. E.; Nilsson, M., *Inducing high linear energy transfer radiolytic degradation using the UCI TRIGA reactor*, Test, Research, and Training Reactors, 2012 Annual Conference, San Diego, CA, USA, Sep 24 – 27, 2012.
24. Pearson, J.; Jan, O.; Miller, G. E.; Nilsson, M., *A comparison of low and high LET (Linear Energy Transfer) induced radiolysis of solvent extraction processes*, ATALANTE Conference, 2012: Nuclear Chemistry for Sustainable Fuel Cycles, French Atomic Energy Commission (CEA), Montpellier, France, Sep. 2- 7, 2012.
25. Mezyk, S.P.; Mincher, B.J.; Martin, L.R., *Radiation-induced radical degradation kinetics of separations ligands,* 244th American Chemical Society Meeting, Philadelphia, PA, Aug 19-23, 2012.
26. Mezyk S.P., *Recycling Spent Nuclear Fuel to Reduce Waste: Radiation Effects on Solvent Extraction Ligands*. Gordon Research Conference on Radiation Chemistry, NH, July 29 – Aug 03, 2012.
27. Pearson, J.; Jan, O.; Miller, G.; Nilsson, M., *High linear energy transfer (LET) induced radiolysis of solvent extraction reagents for nuclear fuel processes via the $^{10}B(n,\alpha)^{7}Li$ reaction*, 20th International Conference On Nuclear Engineering, ICONE 20, Anaheim, CA, USA, July 20- Aug 02, 2012.
28. Pearson, J.; Miller, G.E.; Nilsson, M., *A comparison of low linear energy transfer (LET) vs. high linear energy transfer radiolytic destruction of the extraction ligand tributyl phosphate*, 36th Annual Actinide Separations Meeting, Chattanooga, TN, USA, May 21 – 24, 2012.
29. Mezyk, S.P.; Cullen, T. D.; Mincher, B.J.; Nilsson, M., *Alpha and gamma radiolysis of nuclear solvent extraction ligands used for An(III) and Ln(III) separations*. MARC IX: Ninth International Conference on Methods and Applications of Radioanalytical Chemistry, Mar. 25 – 30, 2012.
30. Pearson, J.; Jan, O.; Miller, G. E.; Nilsson, M., *High linear energy transfer (LET) induced radiolysis of the extraction ligand tributyl phosphate via the $^{10}B(n,\alpha)^{7}Li$ reaction*, 243rd ACS National Meeting, San Diego, CA, USA, Mar 25 – 29, 2012.
31. Pearson, J.; Jan, O.; Luc, W.; Miller, G. E.; Nilsson, M., *Alternative methods for degradation studies by alpha radiolysis*, Tokyo Tech. Weekend Seminar Series, Tokyo University of Technology, Tokyo, Japan, December 18, 2011.
32. Pearson, J.; Jan, O.; Luc, W.; Miller, G. E.; Nilsson, M., *Alternative methods for degradation studies by alpha radiolysis*, Global 2011: Toward and Over the Fukushima Daiichi Accident, Makuhari, Japan, Dec 11 – 16, 2011.
33. Mezyk, S.P., *Radiolytic stability of nuclear reprocessing extraction ligands,* XIX International Solvent Extraction Conference, Santiago, Chile, Oct 3-7, 2011.
34. Mincher, B.J.; Mezyk, S.P.; Elias, G.; Groenwold, G.S., *Radiation chemistry effects on nuclear solvent extraction: Examples from CMPO radiolysis.* 14th International Congress of Radiation Research Warsaw, Poland, Aug 28- Sep 01, 2011.
35. Elias, G.; Groenwold, G.S.; Mincher, B.J.; Mezyk, S.P., *Analytical techniques to detect and quantify CMPO and its radiolytic products*, 242nd American Chemical Society Meeting, Denver, CO, Aug 28 - Sep 01, 2011.

36. Gaskins, D.K.; Cullen, T.D.; Mezyk, S.P.; Martin, L.R., *Investigation into the radiolytic stability of lantahanide-complexed extraction ligands*, 242nd American Chemical Society Meeting, Denver, CO, Aug 28 - Sep 01, 2011.
37. Pearson, J; Jan, O.; Wariner, A.; Dennison, P.; Shaka, A. J.; Miller, G. E.; Nilsson, M., *Development of a method for in-situ alpha radiolysis studies*, American Nuclear Society Summer Meeting, Hollywood, FL, USA, Jun. 26 – 30, 2011.

Student theses:

1. Mr. Thomas Cullen, *Hydroxyl Radical Reaction and Lanthanide Complexation Kinetics of DTPA.* MS Thesis, California State University at Long Beach, 2011 – 2013,
2. Mr. Jeremy Pearson, *High Linear Energy Transfer Radiolysis of Solvent Extraction Ligands.* PhD Thesis, University of California, Irvine, 2010 - 2014,

Research student advisor - Mikael Nilsson:

June 2013 - June 2014, Donald Morrow

June 2014 - August 2014, Julia Bravo, Exchange student, Brazil Scientific Mobility Program.

March 2012 - August 2013, Andrew Clark

June 2010 - August 2012, Oliver Jan

June 2011 - August 2011, Alicia Wariner

Research student advisor – Stephen Mezyk:

Jan 2013 – Dec 2013, Matthew Chagnon

Aug 2012 – Dec 2012, Lauren Olson

Jan 2012 – May 2012, Shauna Otto

Oct 2010 – Dec 2011, Delora Gaskins